

NASA TECHNICAL NOTE



NASA TN D-6113

C.1

NASA TN D-6113

LOAN COPY: RE
AFWL (DC
KIRTLAND AF

0133236



TECH LIBRARY KAFB, NM

TO

A STATISTICAL STUDY OF ABILITY OF SIMULATED PILOTS TO CONTROL THE APPROACH AND DESCENT OF THE LUNAR MODULE TO THE LUNAR SURFACE

by Jacob H. Lichtenstein
Langley Research Center
Hampton, Va. 23365





0133236

1. Report No. NASA TN D-6113		2. Government Accession No.		3. Recipient's Catalog No.	
4. Title and Subtitle A STATISTICAL STUDY OF ABILITY OF SIMULATED PILOTS TO CONTROL THE APPROACH AND DESCENT OF THE LUNAR MODULE TO THE LUNAR SURFACE				5. Report Date March 1971	
				6. Performing Organization Code	
7. Author(s) Jacob H. Lichtenstein				8. Performing Organization Report No. L-7377	
9. Performing Organization Name and Address NASA Langley Research Center Hampton, Va. 23365				10. Work Unit No. 127-51-34-03	
				11. Contract or Grant No.	
12. Sponsoring Agency Name and Address National Aeronautics and Space Administration Washington, D.C. 20546				13. Type of Report and Period Covered Technical Note	
				14. Sponsoring Agency Code	
15. Supplementary Notes					
16. Abstract An analytical study was made to assess the ability of a pilot, simulated by permissible error performance, to control the entire lunar approach and descent with relatively simple guidance schemes. The control task consisted of applying retrothrust during the hyperbolic approach to establish a lunar orbit. During this lunar coasting orbit, the lunar module was separated from the command and service module. A second deorbit thrust period was used on the lunar module to establish a coasting descent, and a final thrust period was used to put the vehicle into a reasonable landing situation. Throughout the maneuver the pilot was permitted to make reasonable errors, selected in a random manner, in the thrust time and attitude control. The control schemes consisted of maintaining a constant vehicle attitude with respect to the line of sight to the lunar horizon for the first and second thrust periods, and a constant angle with respect to the line of sight to the orbiting command and service module for the third thrust period. The results show that a relatively accurate pilot, one whose standard deviation of error is 0.1 sec and 0.1° or less, would be necessary to avoid excessively large errors. Even such a pilot would be required to switch to another form of terminal guidance to bring the flight conditions within acceptable values near touchdown. Correction coefficients were determined which permitted corrections to be applied to the second and third thrust periods for errors made in the previous thrust periods. When these correction coefficients were applied, the final standard error in altitude for the worst pilot was reduced from about 25 000 to 3000 ft (7620 to 914 m) and the number of impacts with the ground was reduced from 21 to 2 in the total of 51 runs.					
17. Key Words (Suggested by Author(s)) Simulated pilots Statistical study of pilots' ability Control of lunar approach and descent			18. Distribution Statement Unclassified - Unlimited		
19. Security Classif. (of this report) Unclassified		20. Security Classif. (of this page) Unclassified		21. No. of Pages 57	
				22. Price* \$3.00	

A STATISTICAL STUDY OF ABILITY OF SIMULATED PILOTS TO CONTROL THE APPROACH AND DESCENT OF THE LUNAR MODULE TO THE LUNAR SURFACE

By Jacob H. Lichtenstein
Langley Research Center

SUMMARY

An analytical study was made to assess the ability of a pilot, simulated by permissible error performance, to control the entire lunar approach and descent with relatively simple guidance schemes. The control task consisted of applying retrothrust during the hyperbolic approach to establish a lunar orbit. During this lunar coasting orbit, the lunar module was separated from the command and service module. A second deorbit thrust period was used on the lunar module to establish a coasting descent, and a final thrust period was used to put the vehicle into a reasonable landing situation. Throughout the maneuver the pilot was permitted to make reasonable errors, selected in a random manner, in the thrust time and attitude control. The control schemes consisted of maintaining a constant vehicle attitude with respect to the line of sight to the lunar horizon for the first and second thrust periods, and a constant angle with respect to the line of sight to the orbiting command and service module for the third thrust period.

The results show that a relatively accurate pilot, one whose standard deviation of error is 0.1 sec and 0.1° or less, would be necessary to avoid excessively large errors. Even such a pilot would be required to switch to another form of terminal guidance to bring the flight conditions within acceptable values near touchdown.

Correction coefficients were determined which permitted corrections to be applied to the second and third thrust periods for errors made in the previous thrust periods. When these correction coefficients were applied, the final standard error in altitude for the worst pilot was reduced from about 25 000 to 3000 ft (7620 to 914 m) and the number of impacts with the ground was reduced from 21 to 2 in the total of 51 runs.

INTRODUCTION

Simple techniques for guidance, navigation, and control are of interest in space flight as a means of reducing hardware complexity or for use in manual backup modes. Much work has been done in this area at the NASA Langley Research Center as well as

in various other organizations (see refs. 1 to 6, for example). In most studies of this type individual tasks have been considered, either analytically or by simulation. Such tasks have included establishment of lunar orbits, lunar landings, rendezvous, and launch from the moon. The control tasks in each of these phases have involved orientation of the spacecraft and application of a specified thrust level for some time interval. The analyses of references 1 to 6 have indicated that simple visual cues, such as views of the lunar horizon or of an orbiting spacecraft, could be used for spacecraft orientation during the thrusting periods. The analyses have also indicated that the various thrusting phases could be accomplished quite accurately and economically.

The purpose of the present study was to examine analytically how well a pilot, using the simplified guidance techniques suggested in the references mentioned previously, can perform the sequential tasks required during the lunar landing mission. This mission starts with the spacecraft approaching the moon in a hyperbolic orbit and terminates with the lunar module close to touchdown. The tasks required of the pilot are to control the vehicle thrust in order to (a) establish a near-circular coasting orbit, (b) brake from the coasting orbit into a descent transfer orbit, and (c) brake from the transfer orbit to the final near-touchdown conditions. This sequence of events is shown in figure 1. Since statistical experimental error data for pilots performing the required tasks for the entire trajectory are not available, a mathematical model representing the pilots was required. This model was defined by the magnitude of the errors in thrust control angle and in the response times for the start and stop of thrust. Eighteen pilots were represented by various combinations of the magnitudes of the angle and time errors. Statistical data were obtained by making 51 complete runs for each pilot, with the actual magnitudes of the errors selected by a Monte Carlo technique.

Since it was recognized that the pilot would make control errors during the descent and that the final altitude error may be quite large, some method of compensating for the errors may be required. Therefore, a set of error coefficients was developed which would indicate the changes to be made during the second and third thrust periods to compensate for errors made in the previous thrust periods.

SYMBOLS

In this investigation, measurements were made in U.S. Customary Units but they are also given in the International System of Units (SI). The symbols used in this report are defined as follows:

- | | |
|---|--|
| A | average value of a parameter, $\frac{\sum P}{n}$ |
| C | correct value of a parameter obtained from nominal run |

$$G = \frac{\mu M}{R^2}$$

h	altitude above the lunar surface, ft (m)
l	distance between the LM and the CSM, ft (m)
M	mass of the moon, slugs (kg)
m	mass of the vehicle, slugs (kg)
m_0	initial mass of the vehicle, slugs (kg)
n	number of measurements of the parameter under consideration
P	value of the parameter under consideration
R	radius from the center of the moon to the vehicle, n. mi. or ft (m)
R_0	radius of the moon, 5 702 000 ft (1 737 969.6 m)
S	standard error of a parameter, $\sqrt{\frac{\sum (P - C)^2}{n}}$
t	time, sec
t_0	time at start of computations (at $h = 200$ n. mi. or 370 400 m)
t_1	time at start of first thrust period, sec
t_2	time at end of first thrust period, sec
t_3	time at start of second thrust period, sec
t_4	time at end of second thrust period, sec
t_5	time at start of third thrust period, sec
t_6	time at which the vehicle reaches minimum altitude, sec
t_7	time at which the vehicle reaches the moon's surface, sec

Δt_I	error in the length of the first thrust period, sec
Δt_{II}	error in the length of the second thrust period, sec
Δt_{III}	time error at the start of the third thrust period, sec
V	velocity of the vehicle, ft/sec (m/sec)
X_i, Y_i	inertial axes (see fig. A-1(b))
x_i, y_i	distances along X_i and Y_i axes, respectively, ft (m)
X, Y, Z	body axes of the vehicles, oriented as shown in figure 2, with the subscript denoting the vehicle
α	angle between the local vertical and the line of sight from the LM to the CSM, deg
γ	flight-path angle, measured up from the local horizontal, deg
η_1	angle between the line of sight from the CSM to the trailing lunar horizon and the X_{CSM} axis during first thrust, deg
η_2	angle between the line of sight from the LM to the trailing lunar horizon and the X_{LM} axis during second thrust, deg
θ	angular displacement of the vehicle in the $X_i Y_i$ plane, $\tan^{-1} \frac{y_i}{x_i}$, rad
λ	longitude on the lunar surface, deg
μ	universal gravitational constant, $6.668 \times 10^{-23} \frac{\text{km}^3}{\text{g sec}^2}$
ξ	angle between the X body axis and the local horizontal, deg
σ	standard deviation of a parameter, $\sqrt{\frac{\sum (P - A)^2}{n - 1}}$
τ	angle between the local vertical and the line of sight to the lunar horizon, deg

ν angle between the line of sight from the LM to the CSM and the X_{LM} axis,
deg

Subscripts:

A altitude

a control angle

CSM command and service module

LM lunar module

$R_0\theta$ range

t time

V velocity

Dots above a symbol denote differentiation with respect to time.

METHOD

The analysis and results of this paper are based on the computed ability of pilots to fly along a predetermined nominal trajectory by adhering to a time-defined nominal flight plan. It is assumed that the spacecraft is approaching the moon along a hyperbolic trajectory similar to that for the Apollo mission, and the nominal trajectory starts at an altitude of 200 n. mi. (370 400 m) above the surface. The terminal conditions are an altitude of 1 n. mi. (1852 m), zero vertical velocity, and a forward velocity of about 600 ft/sec (182.9 m/sec). In order to obtain data for the statistical analysis, 51 descent trajectories in which the control errors were randomly selected were computed for each of the 18 pilots considered.

The trajectory computations were made by using a general three-degree-of-freedom system of equations with the moon as the central body. For this investigation, however, it was decided that there would be no loss in generality if the problem were restricted to the planar case with the vehicle free to move longitudinally and vertically and to rotate for thrust alinement. The computations permit controlled thrust of the combined vehicle (command and service module with attached lunar module) during its approach, separation of the two vehicles, and thrust of the lunar module while keeping track of the orbiting command and service module. Because this was a general investigation, no attempt was

made to duplicate a specific Apollo mission, in which the lunar horizon may not be visible. For this investigation, it was assumed that the lunar horizon would be visible and that there would be no uncertainty in horizon determination due to terrain irregularities. A more detailed discussion of the equations used during the pilot control part of the experiment is presented in appendix A. A separate computational program was used to reduce the resulting statistical data and to make the plots of these data.

Nominal Flight Path

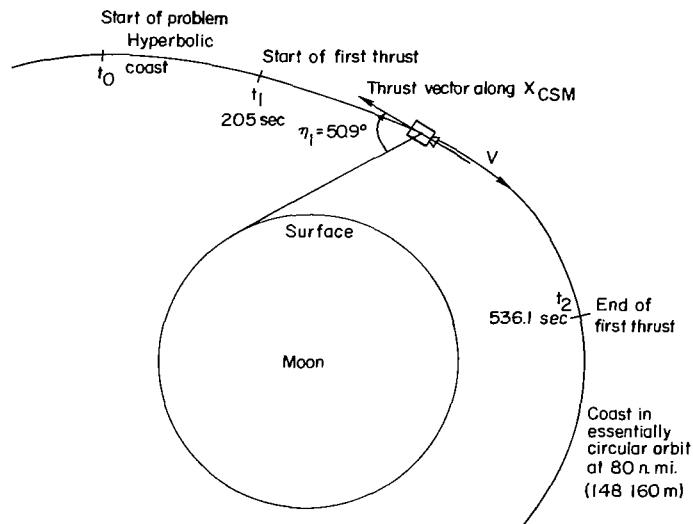
The nominal flight path was determined by an iteration procedure which resulted in the desired trajectory characteristics at key phases of the mission. This trajectory was designed to allow manual control of the approach, and no attempt was made to duplicate the present Apollo approach. The nominal trajectory starts at 200 n. mi. (370 400 m) along the hyperbolic approach, and at that point it has the following parameters:

$$V = 7945.04 \text{ ft/sec (2421.65 m/sec)}$$

$$\gamma = -20.722\ 936\ 5^\circ$$

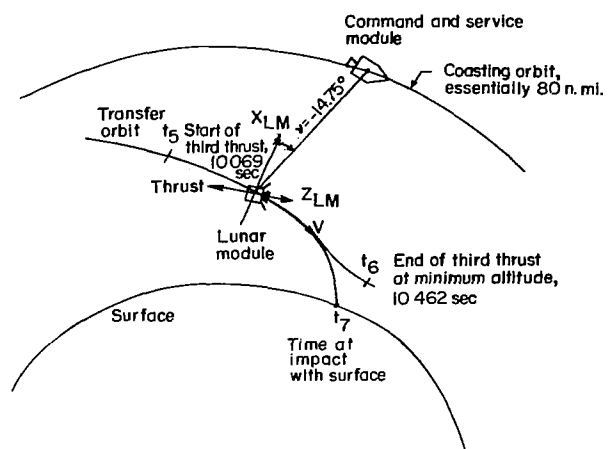
$$h = 1\ 215\ 406.2 \text{ ft (370\ 455.8 m)}$$

Three thrust periods are used to accomplish the mission. The first slows the combined vehicle from the approach velocity and establishes a nearly circular orbit at 80 n. mi. (148 160 m). The second slows the lunar module from orbital velocity to establish a descent transfer orbit with periapsis at 50 000 ft (15 240 m). The third is the final slow-down to the terminal conditions. These thrusting tasks are depicted in figure 1. The body axes of the vehicles are oriented as shown in figure 2.



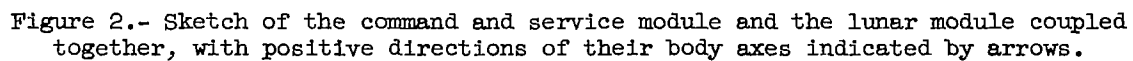
(a) Establishment of circular orbit.

Figure 1.- The three thrusting tasks required of the pilot.



(c) Landing approach.

Figure 1.- Concluded.



In order to follow this trajectory the pilot's mission time schedule is as follows:

$$t_0 = 0.000 \text{ sec}$$

Problem is initiated at 200 n. mi. (370 400 m). Remain in the coasting orbit.

$$t_1 = 205.000 \text{ sec}$$

Aline the vehicle so that the X_{CSM} axis is at an angle of 50.9° with the receding lunar horizon (see fig. 1(a)). Initiate thrust and maintain until t_2 .

$$t_2 = 536.100 \text{ sec}$$

End thrust. Vehicle should now be in a nearly circular coasting orbit at 80 n. mi. (148 160 m).

$$t_2 \text{ to } t_3$$

Coast in nearly circular orbit, during which separation of LM and CSM occurs.

$$t_3 = 6580.000 \text{ sec}$$

Aline the LM so that the X_{LM} axis is at an angle of 67.15° with the receding lunar horizon (see fig. 1(b)), and initiate thrust in the LM. This time was chosen because it is at the periapsis of the nearly circular orbit.

$$t_4 = 6589.445 \text{ sec}$$

End thrust. The LM should be in a descending transfer orbit.

$$t_4 \text{ to } t_5$$

Coast in transfer orbit

$$t_5 = 10\,069.000 \text{ sec}$$

Aline LM so that the X_{LM} axis is at an angle of -14.75° with the line of sight to the orbiting CSM and start thrust (see fig. 1(c)). Maintain this angle throughout the thrust period. This time was chosen because it is the periapsis of the transfer orbit at $h = 50\,761 \text{ ft}$ (15 472 m).

$$t_6 = 10\,462 \text{ sec}$$

End thrust. The LM should be at the terminal conditions:

$$h = 6465 \text{ ft (1970.5 m)}$$

$$\dot{h} \approx 0$$

$$V = 549.3 \text{ ft/sec (167.4 m/sec)}$$

These end conditions are similar to those for a medium-speed airplane in level flight, and it is assumed that a pilot with proper training can make a safe landing on the lunar surface.

Pilot Performance Definition

Since this was an analytical study, a definition for the mathematical model of the pilot was required. For any run (single trajectory computation) the magnitude and direction of the possible errors would occur in a random manner. The spectrum of the errors for any task is defined by the error distribution and standard deviation. In this investigation it was assumed that the pilot's errors would be normally distributed about zero. The standard deviations (σ_a and σ_t) were based on some unpublished tests using an engineer as a pilot. These tests were multitask jobs in which the pilot's attention was applied primarily to maintaining three-axis attitude control, and initiation and cutoff of thrust were in response to an audible signal. The results showed that starting and stopping the thrust could readily be controlled to 0.1 sec and the angle could be controlled to within 0.2° . A total of 18 pilot definitions were used in this study, and they are specified in table I in terms of σ_a and σ_t .

TABLE I.- PILOT PERFORMANCE PARAMETERS

Pilot	σ_a , deg	σ_t , sec
1	0	0.05
2	0	.10
3	0	.20
4	.05	0
5	.05	.05
6	.05	.10
7	.10	0
8	.10	.05
9	.10	.10
10	.10	.15
11	.10	.20
12	.15	.10
13	.15	.15
14	.15	.20
15	.20	0
16	.20	.10
17	.20	.15
18	.20	.20

A random-number computing subroutine, called the Monte Carlo technique, was used to obtain the errors at each of the actions required of the pilot. The actual distribution of the errors as they occurred during a typical series of runs ($\sigma_a = 0.20^\circ$, $\sigma_t = 0.20$ sec) is shown in figure 3. In figure 3(a) the number of occurrences of the errors in each magnitude bracket is shown for each time (t_1 , t_2 , etc.) and for the compilation of all five times. Similar data for the angle errors are shown in figure 3(b). Because of the relatively low number of samples (51 runs) at any time point, the error distribution is only approximately normal; however, if all the timing errors for a series (errors at t_1 , t_2 , t_3 , t_4 , and t_5 for all 51 runs) are considered, it can be seen that the error distribution is very close to a normal distribution. The nearly straight line that results when the cumulative percentage total is plotted on probability paper confirms this conclusion.

Vehicle

The vehicles assumed in this investigation were similar to vehicles considered for the Apollo mission. A sketch of the command and service module and the lunar module is shown in figure 2. The mass and thrust magnitude data for the combined vehicle (command and service module with the attached lunar module) were obtained from the Apollo literature available at the time this investigation was started. The values used in this investigation for the combined and lunar modules are:

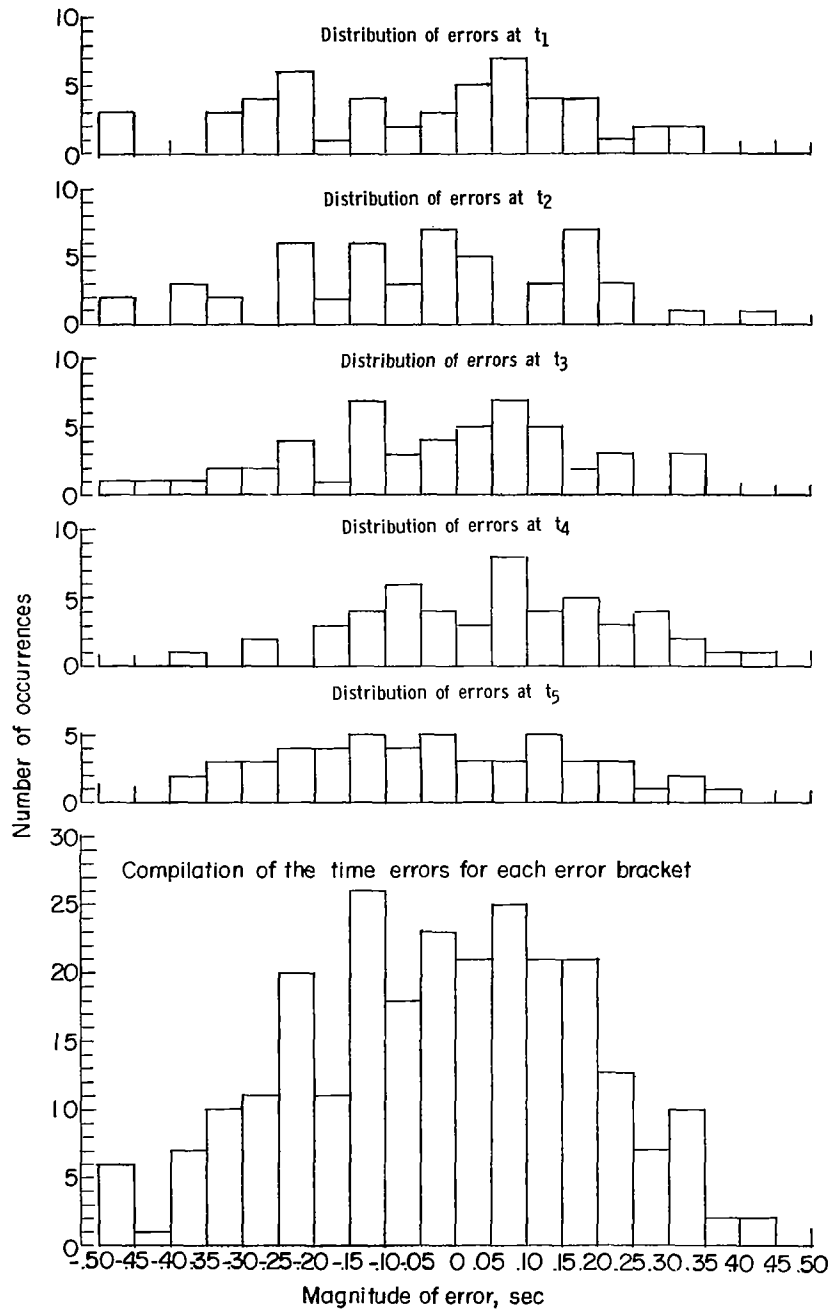
Combined vehicle:

Mass	2741.67 slugs	(40 011.7 kg)
Thrust	21 897 lb	(97 402.7 N)
Mass flow during thrust	2.259 slugs/sec	(33.0 kg/sec)

Lunar module:

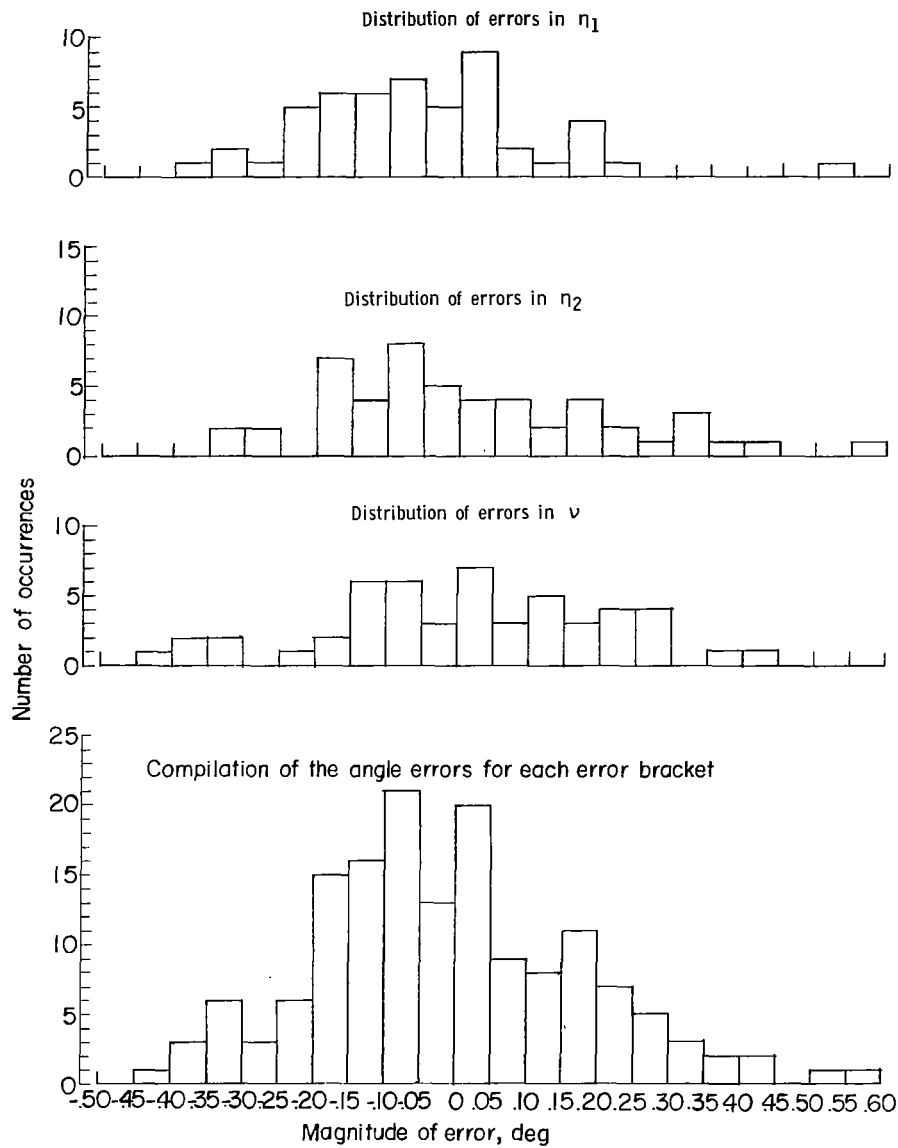
Mass	974.13 slugs	(14 212.6 kg)
Thrust	10 000 lb	(44.482.2 N)
Mass flow during thrust	1.0318 slugs/sec	(15.1 kg/sec)

The direction of thrust is along the X_{CSM} axis in the positive direction for the combined vehicle and along the Z_{LM} axis in the negative direction for the lunar module. Since this investigation was concerned with piloting performance, errors such as thrust misalignment, flow irregularities, and thrust tailoff were not considered.



(a) Distribution of the time errors.

Figure 3.- Typical distribution of the time and angle errors.
This distribution is from pilot 18.



(b) Distribution of the angle errors.

Figure 3.- Concluded.

RESULTS AND DISCUSSION

Standard Flight Procedure

Each computed trajectory was examined at several points to determine departures in altitude, velocity, and range from the nominal trajectory. The points examined were the end of the first and second thrust periods (t_2 and t_4 , respectively) and the start and end of the third thrust period (t_5 and t_6 , respectively). The third thrust period was assumed to terminate either when the rate of descent became zero or on ground contact, whichever occurred first. Examples of the type of data obtained are given in appendix B. These data are in the form of bar graphs showing the distribution of errors in velocity and altitude for the various pilot definitions. The results were compiled in figures 4 to 8 in a form more suitable for analysis. These figures show the effects of pilot definition (σ_a and σ_t) on the magnitude of the standard errors in altitude, velocity, and range.

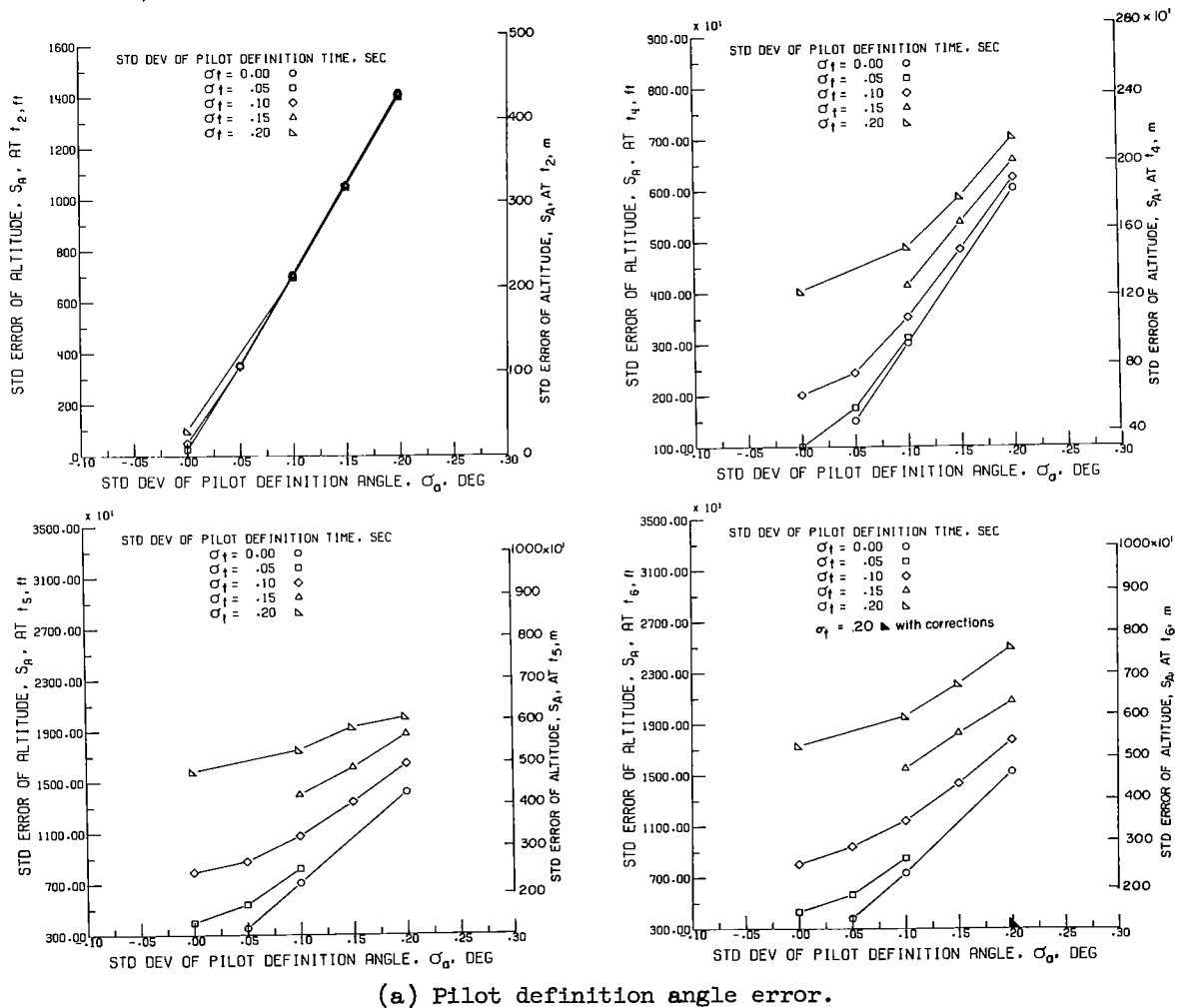
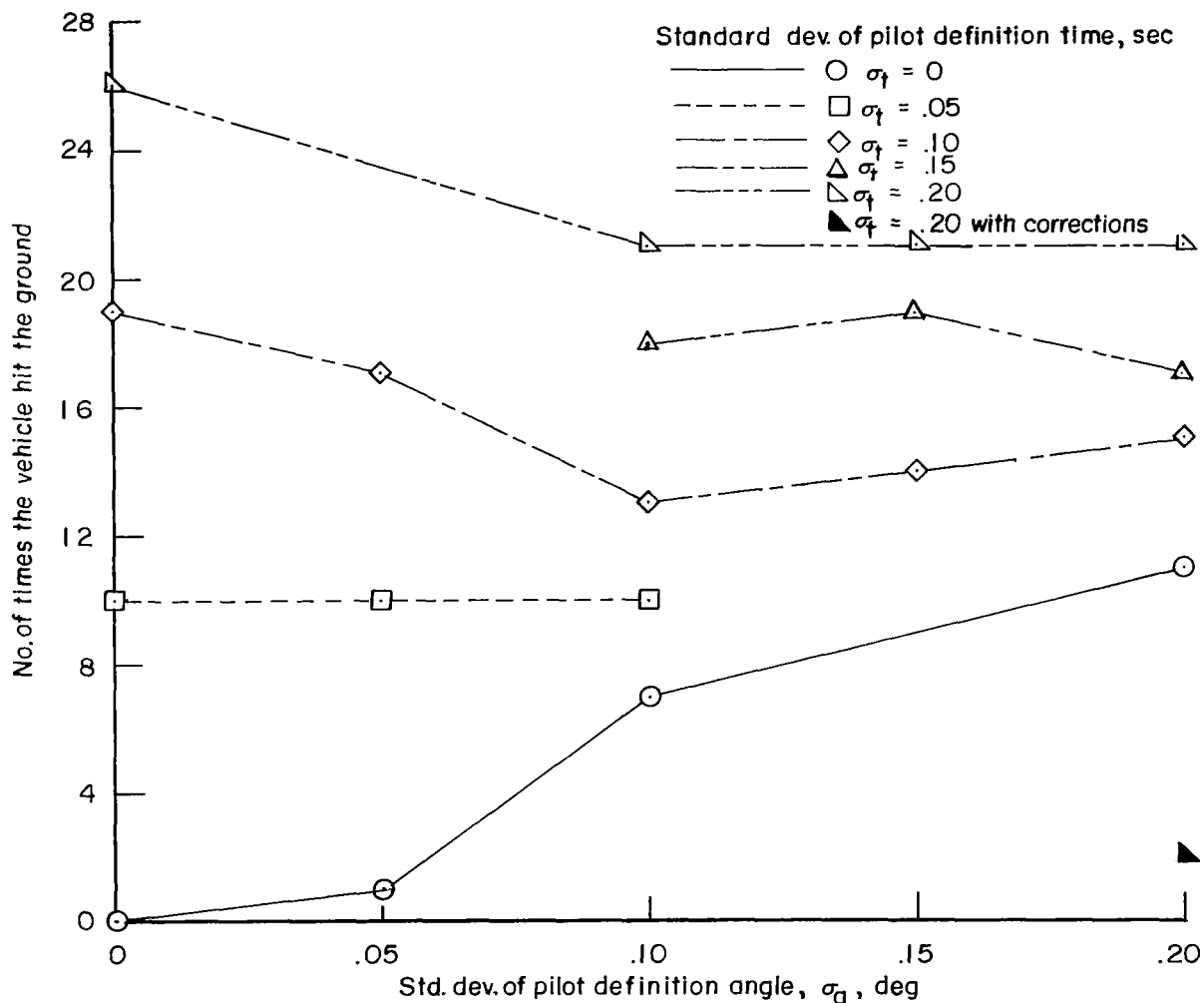


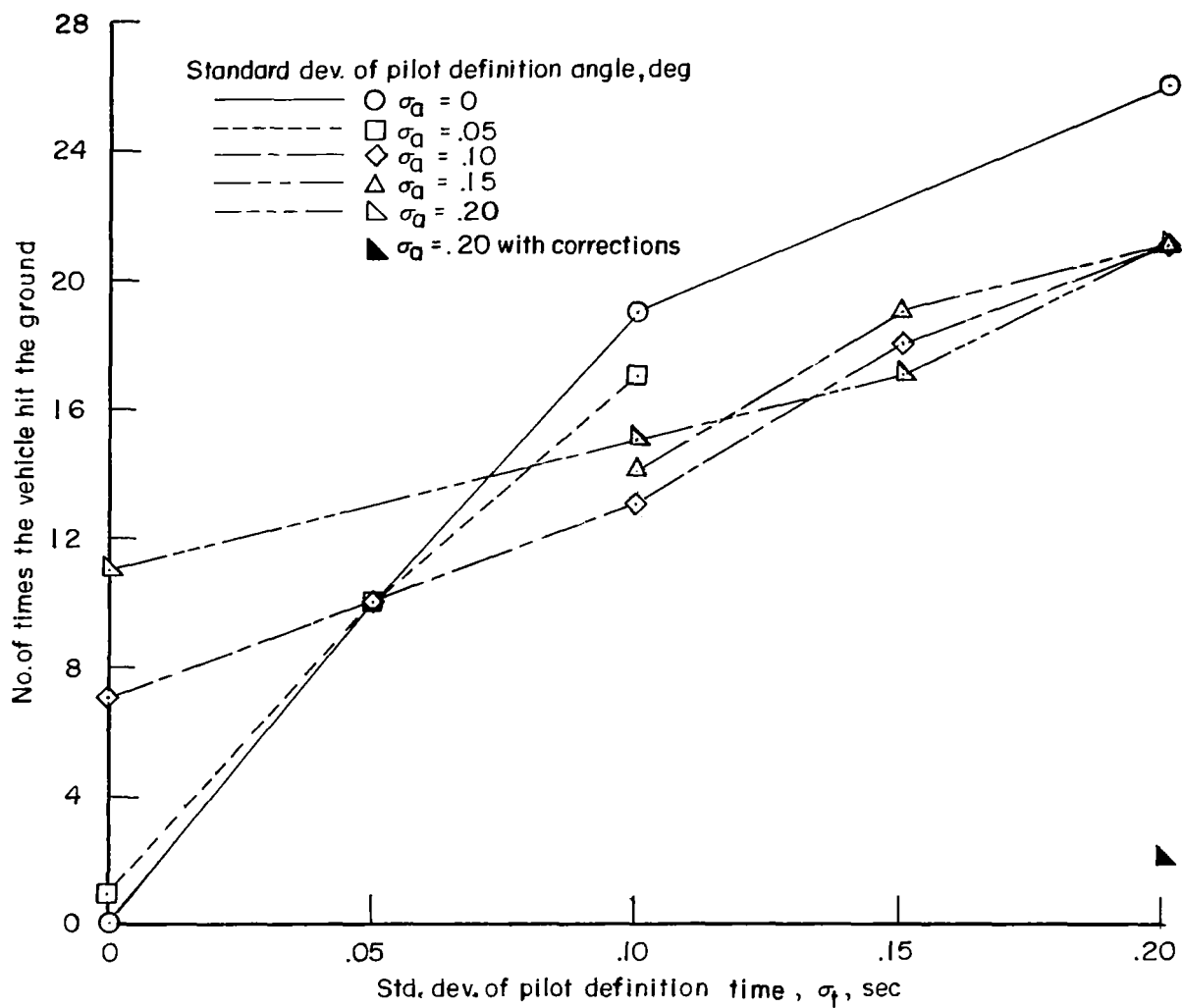
Figure 4.- Variation of the standard error in altitude with pilot definition.

are essentially positive, as large negative errors would cause the vehicle to hit the surface. The seriousness of large negative errors is indicated in figure 5, where each point represents the number of surface impacts out of the 51 runs of a pilot. The data show that 270 of the total of 918 runs, or about 30 percent, hit the ground. Even for relatively small pilot errors (standard deviations of 0.10 or less) there is still about a 20-percent chance of hitting the surface if no correction is made to the flight procedure. The data for the standard error of the vertical velocities at impact, presented in figure 6, show that these velocities approach 300 ft/sec (91.4 m/sec).



(a) Pilot definition angle error.

Figure 5.- Variation of the number of times the lunar module hit the ground with variation in the pilot definition. A total of 51 runs was made for each pilot.



(b) Pilot definition time error.

Figure 5.- Concluded.

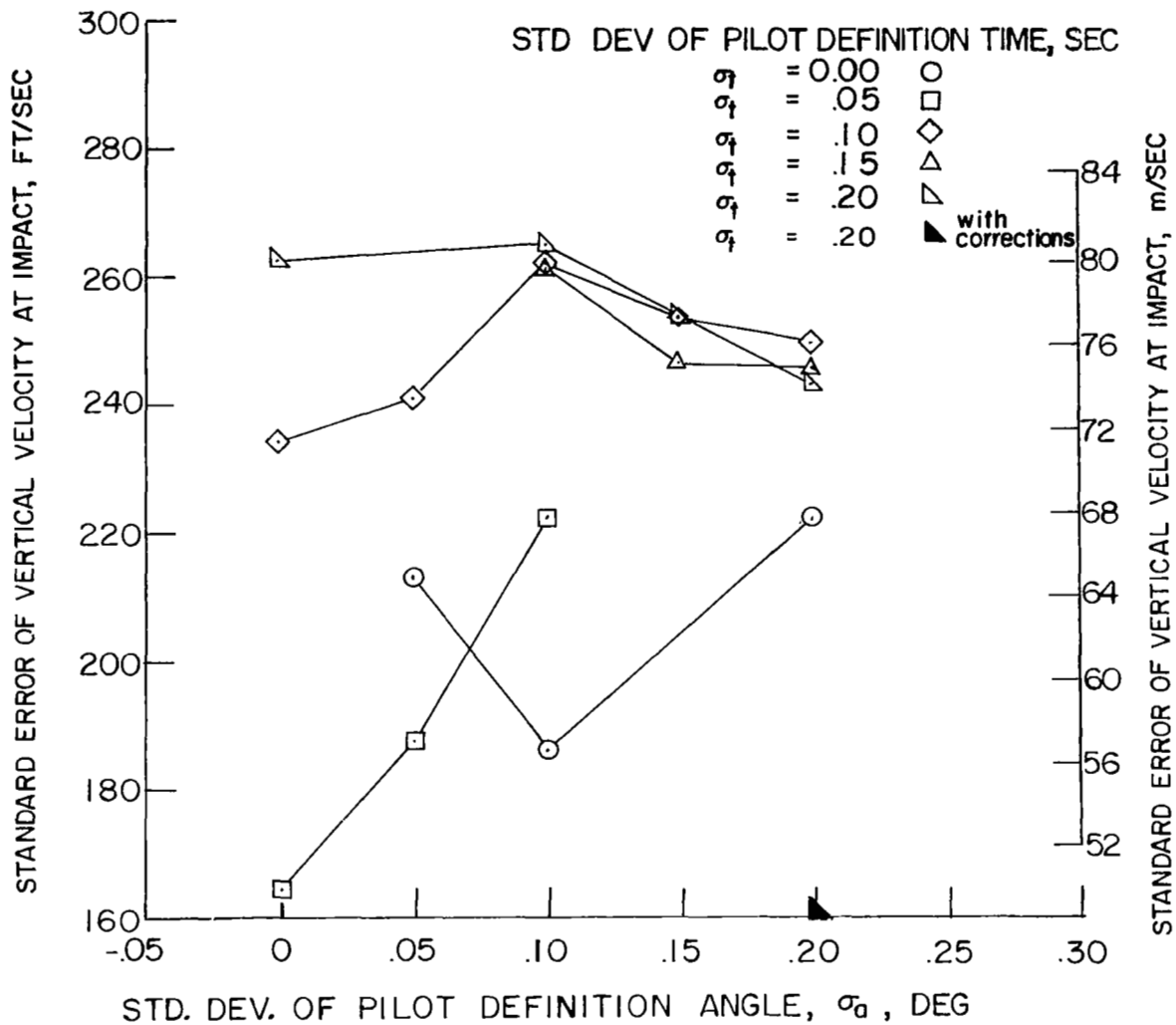
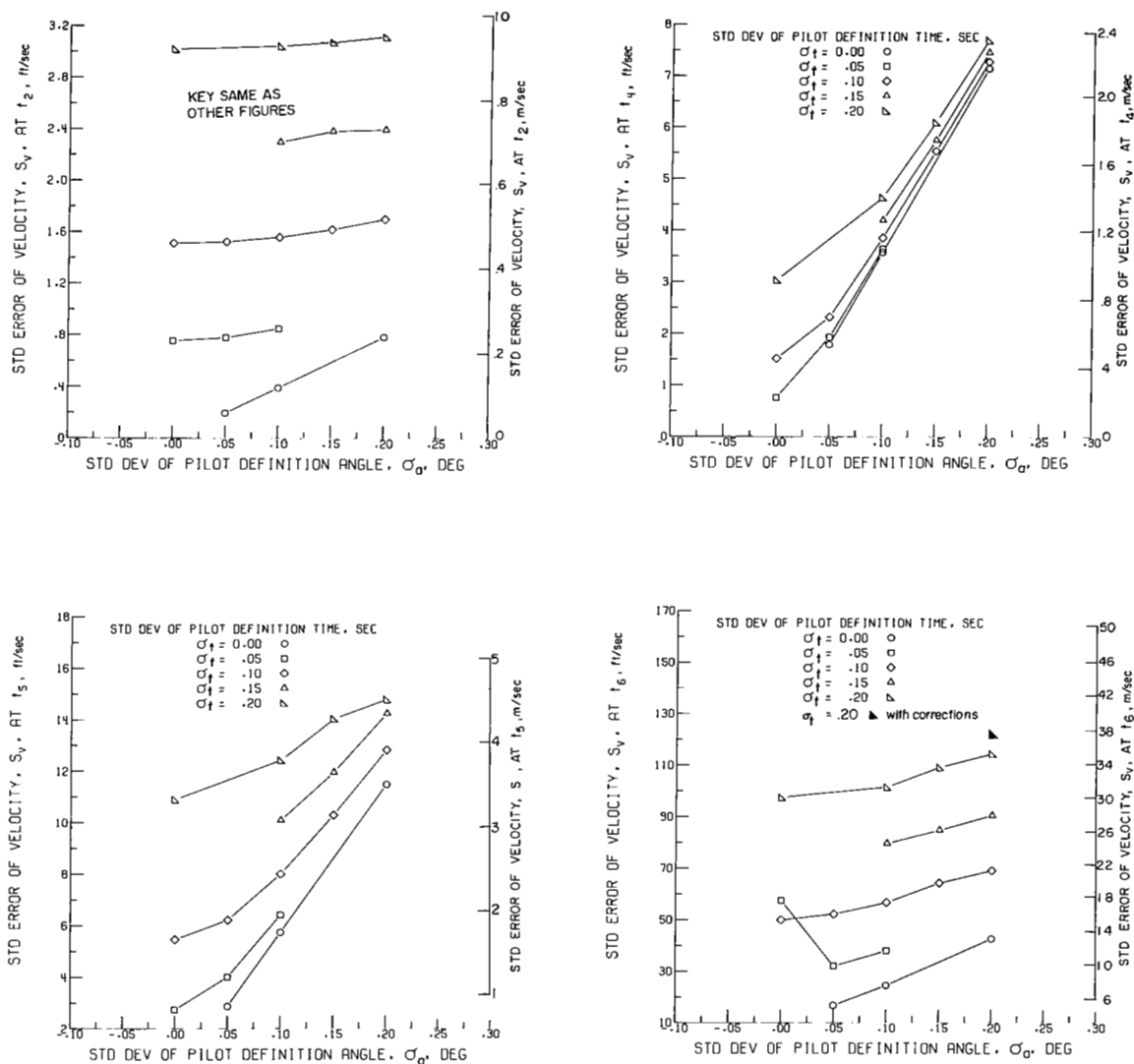


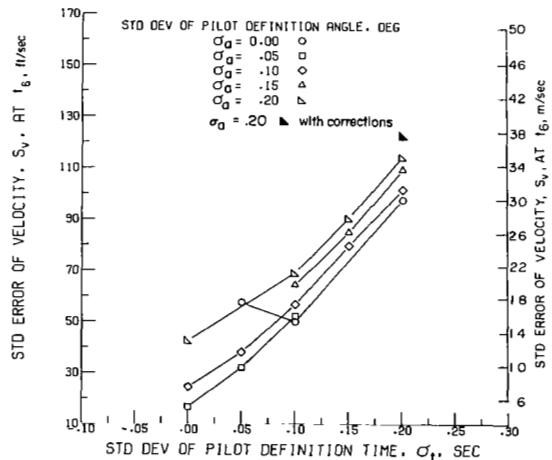
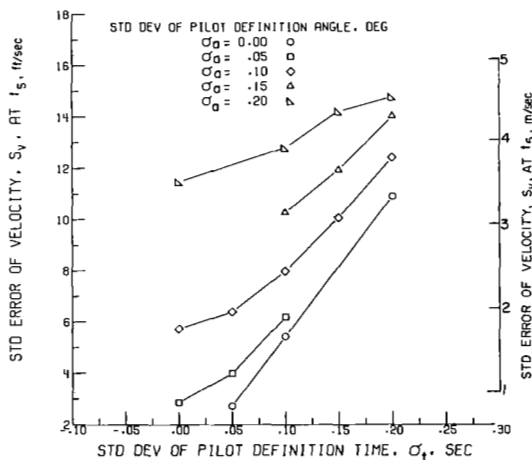
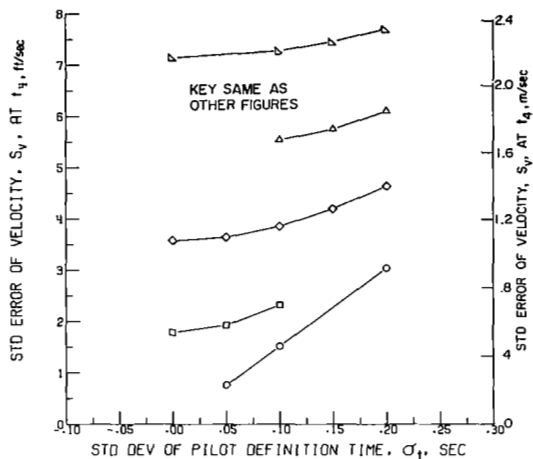
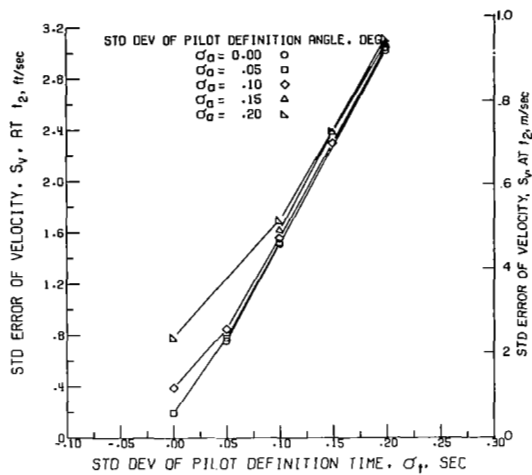
Figure 6.- Vertical velocity at the time of impact with the ground as a function of pilot definition.

Velocity errors. - The buildup of the standard error of the velocity as the trajectories progress is shown in figure 7. The velocity errors are reasonably small even up to the start of landing retrothrust at t_5 , where the error is only 14 ft/sec (4.3 m/sec) at a velocity of 5582 ft/sec (1701.4 m/sec). It is during this last thrust period (between t_5 and t_6) that the largest errors are developed. Note that the data presented at t_6 are for the runs that did not impact, and are thus at minimum altitudes where $\dot{h} = 0$. The errors, therefore, are longitudinal velocity errors.



(a) Pilot definition angle error.

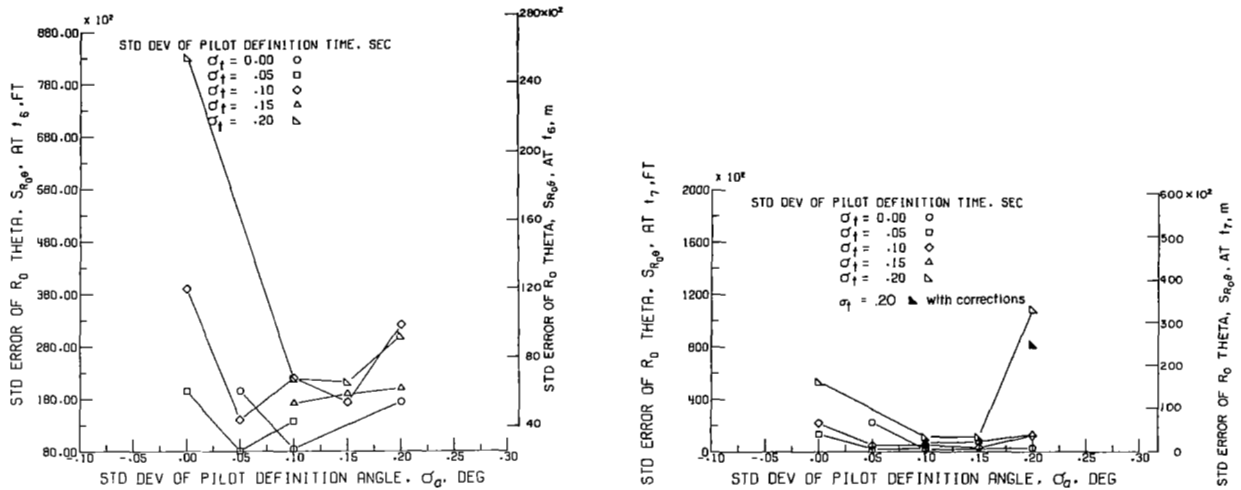
Figure 7.- Variation of the standard error in velocity with pilot definition.



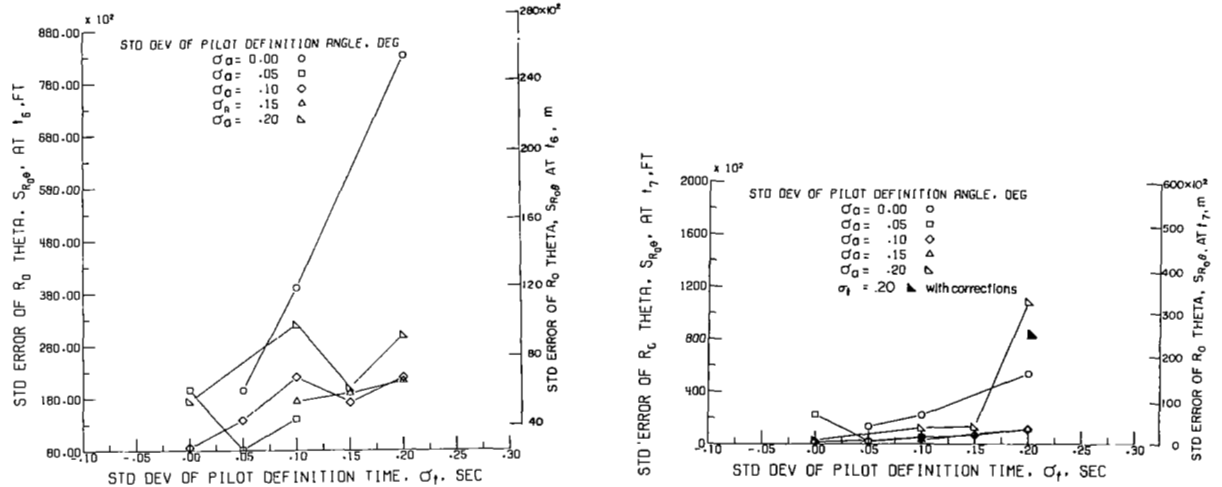
(b) Pilot definition time error.

Figure 7.- Concluded.

Range errors. - The standard errors in range are shown in figure 8. There is not much buildup in range error as time progresses. Most of the error is acquired during the first thrusting period, and generally is less than 5 n. mi. (9260 m).



(a) Pilot definition angle error.



(b) Pilot definition time error.

Figure 8.- Variation of standard error in range with pilot definition.

Correction of Terminal Altitude

Probably the most important conditions to be met in this study are the terminal altitude of about 6500 ft (2000 m) with zero rate of descent. The results of this study indicate the possibility of appreciable departure from these conditions by the assumed pilots following the specified procedure. It is therefore important to obtain, early in the task, some estimate of what the terminal conditions will be, and to correct the trajectory to obtain the desired terminal conditions. This information can be obtained during the relatively long coast times after the first and second thrust periods.

An analytical study was made to determine the effects on the terminal conditions of thrust aiming errors and timing errors for each of the thrust periods individually while the other thrust periods adhered to the nominal plan. The results, presented in figure 9, show that the terminal altitude error is nearly a linear function of the individual errors in angle or time. As a result of this near linearity, the results can be expressed as sensitivity coefficients as follows:

1. Final altitude error per degree of first-thrust angle error (fig. 9(a)):

$$\frac{\partial(\Delta h)}{\partial(\Delta \eta_1)} = -92\,500 \text{ ft/deg } (-28\,194 \text{ m/deg})$$

2. Final altitude error per second of first-thrust time error (fig. 9(b)):

$$\frac{\partial(\Delta h)}{\partial(\Delta t_I)} = -38\,100 \text{ ft/sec } (-11\,612.9 \text{ m/sec})$$

3. Final altitude error per degree of second-thrust angle error (fig. 9(c)):

$$\frac{\partial(\Delta h)}{\partial(\Delta \eta_2)} = -3020 \text{ ft/deg } (-920.5 \text{ m/deg})$$

4. Final altitude error per second of second-thrust time error (fig. 9(d)):

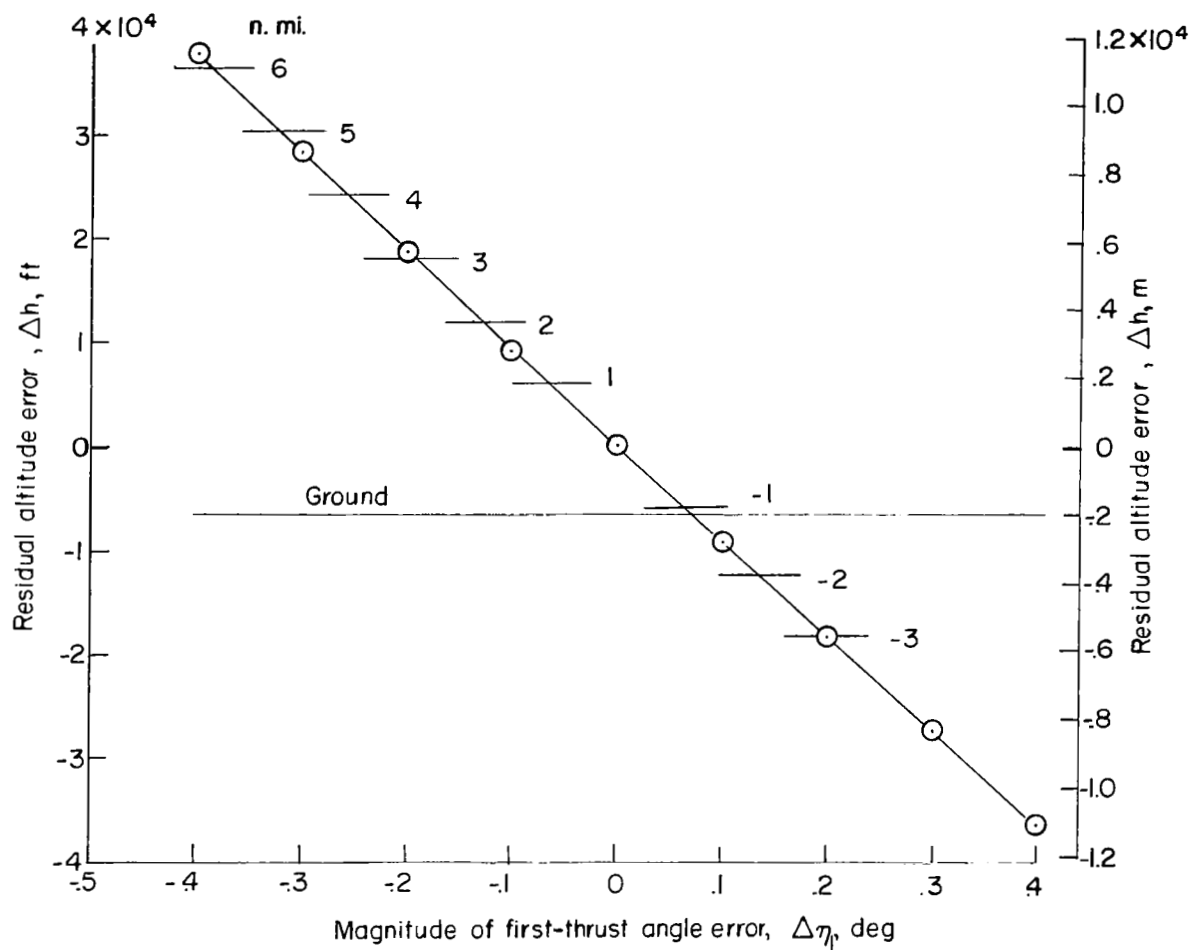
$$\frac{\partial(\Delta h)}{\partial(\Delta t_{II})} = -65\,900 \text{ ft/sec } (-20\,086.3 \text{ m/sec})$$

5. Final altitude error per degree of third-thrust angle error (fig. 9(e)):

$$\frac{\partial(\Delta h)}{\partial(\Delta \nu)} = +14\,200 \text{ ft/deg } (4328.2 \text{ m/deg})$$

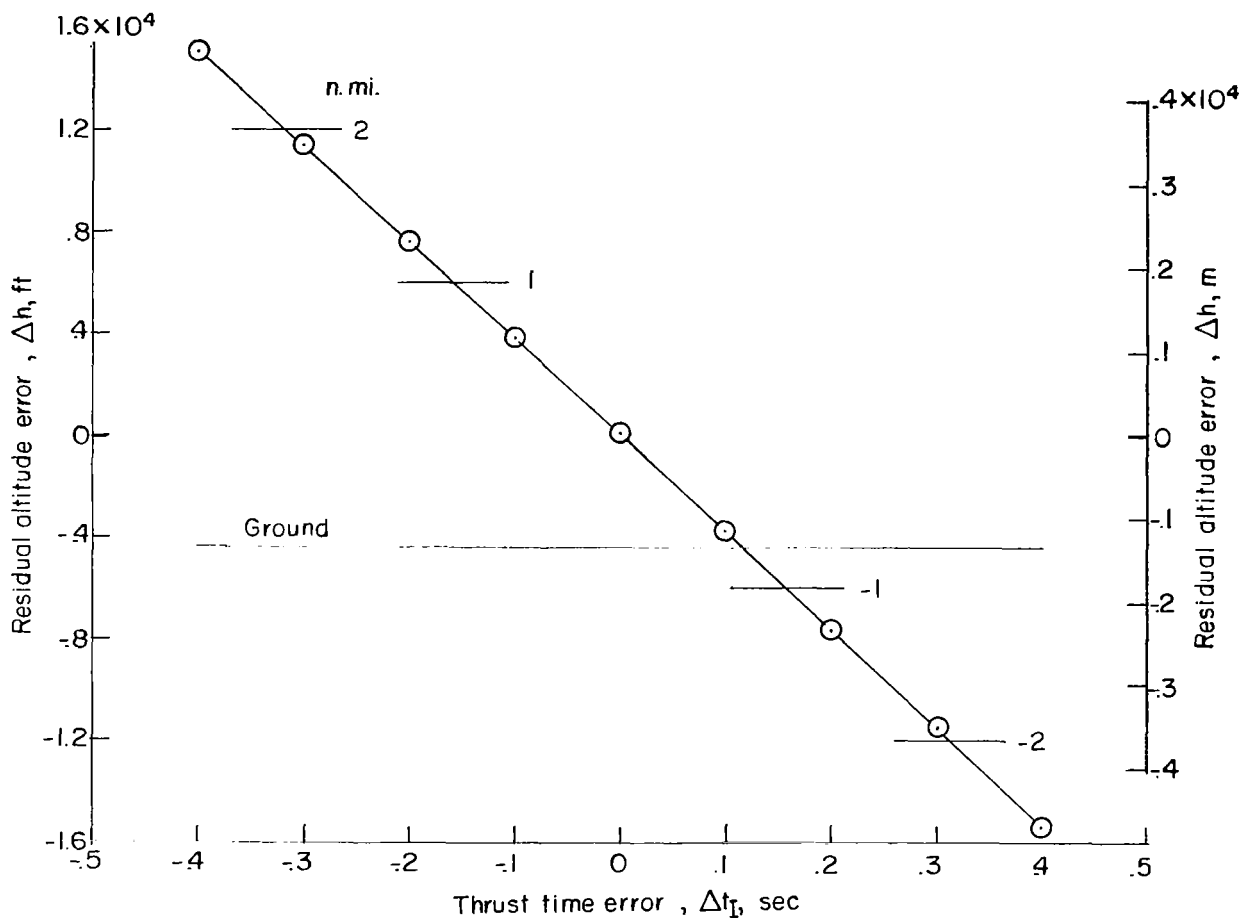
6. Final altitude error per second of time error in starting third thrust:

$$\frac{\partial(\Delta h)}{\partial(\Delta t_{III})} = 251.4 \text{ ft/sec } (76.6 \text{ m/sec})$$



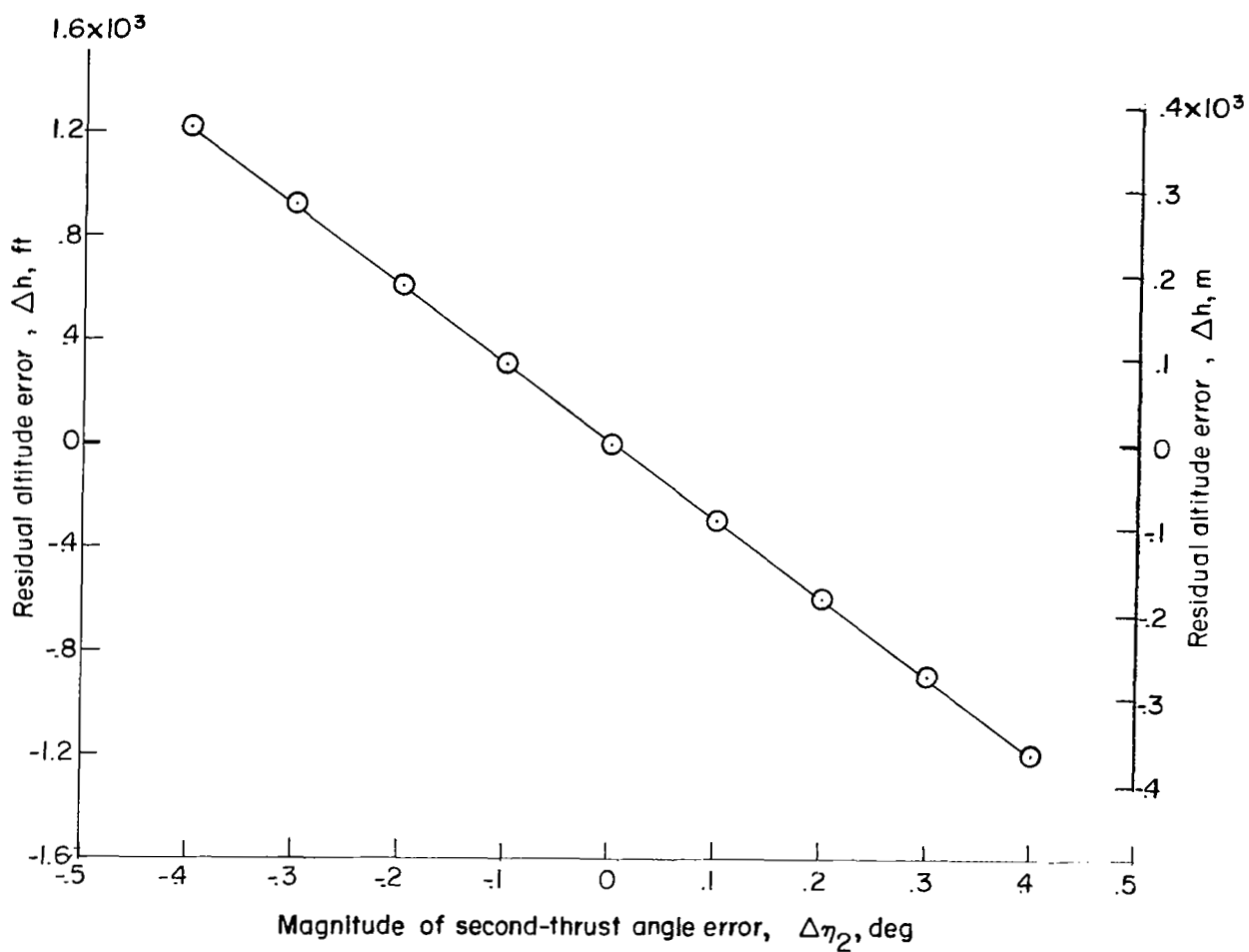
(a) Altitude error due to first-thrust angle error.

Figure 9.- Final altitude error due to the various control errors.



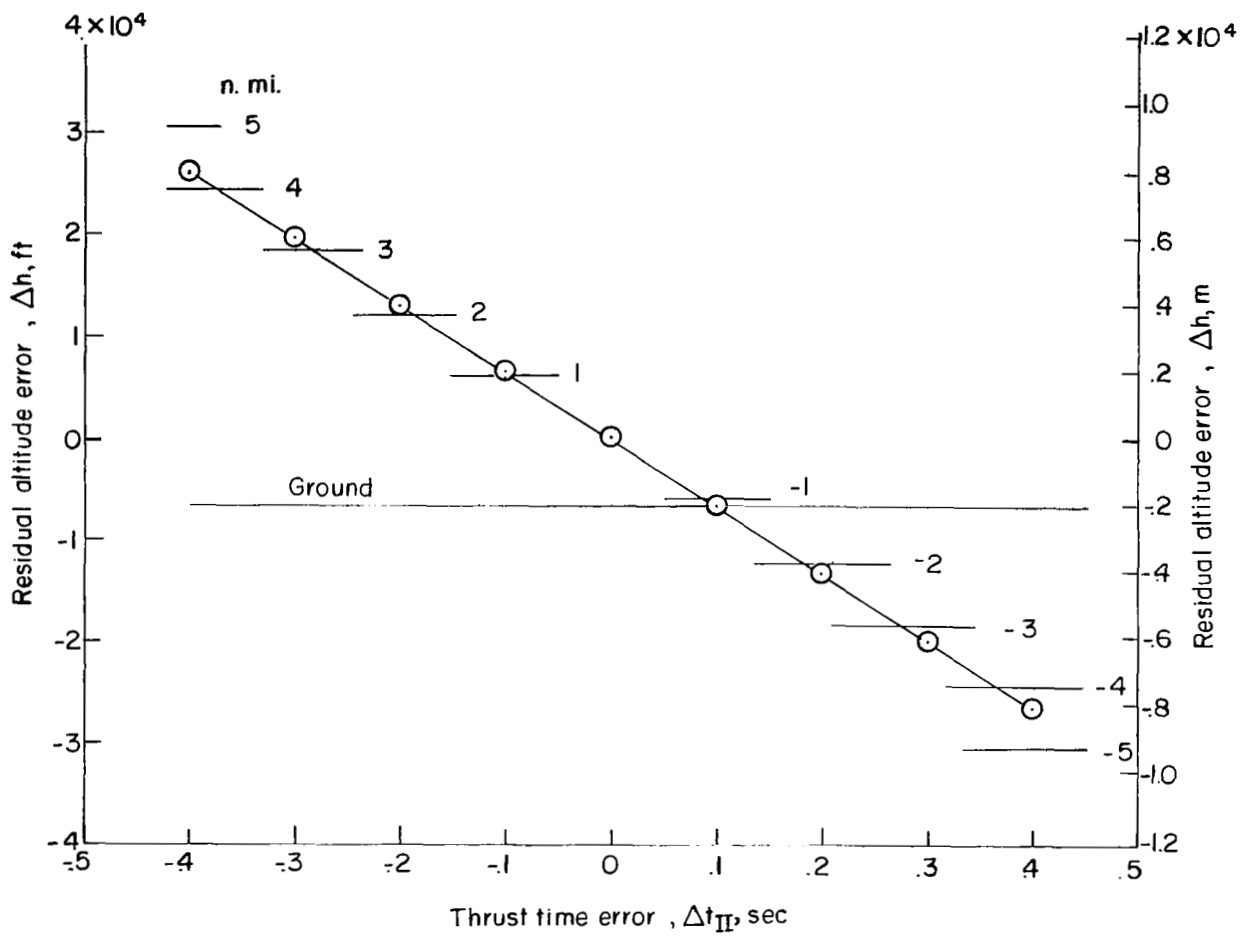
(b) Altitude error due to first-thrust time error.

Figure 9.- Continued.



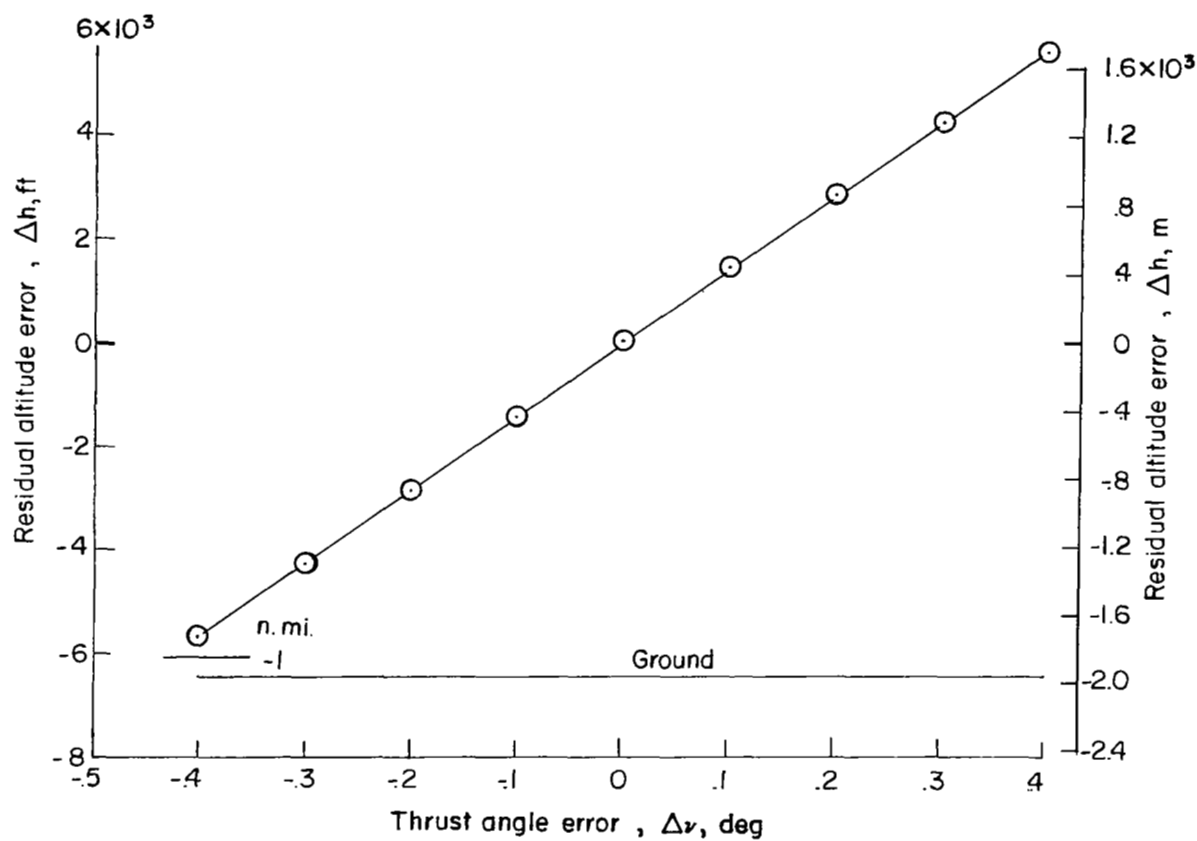
(c) Altitude error due to second-thrust angle error.

Figure 9.- Continued.



(d) Altitude error due to second-thrust time error.

Figure 9.- Continued.



(e) Altitude error due to third-thrust angle error.

Figure 9.- Concluded.

These control coefficients offer a means of rectifying errors made during a thrust period by applying corrective measures in the subsequent thrust periods. If an angle or time error was made during a thrust maneuver, the coefficients could be used to predict the magnitude of the altitude error that would result at the end of the trajectory if the nominal plan is followed. If the magnitude of the error is unacceptable, corrective measures are necessary. By examination of the coefficients for the following thrust periods, the corrections to the angle or time which would be required to compensate for the initial error can be determined. Exact correction of the altitude error probably will not be obtained because the curves in figure 9 are not exactly linear and because the error coefficients were determined as sensitivity parameters about the nominal trajectory, whereas they will be applied to off-nominal conditions.

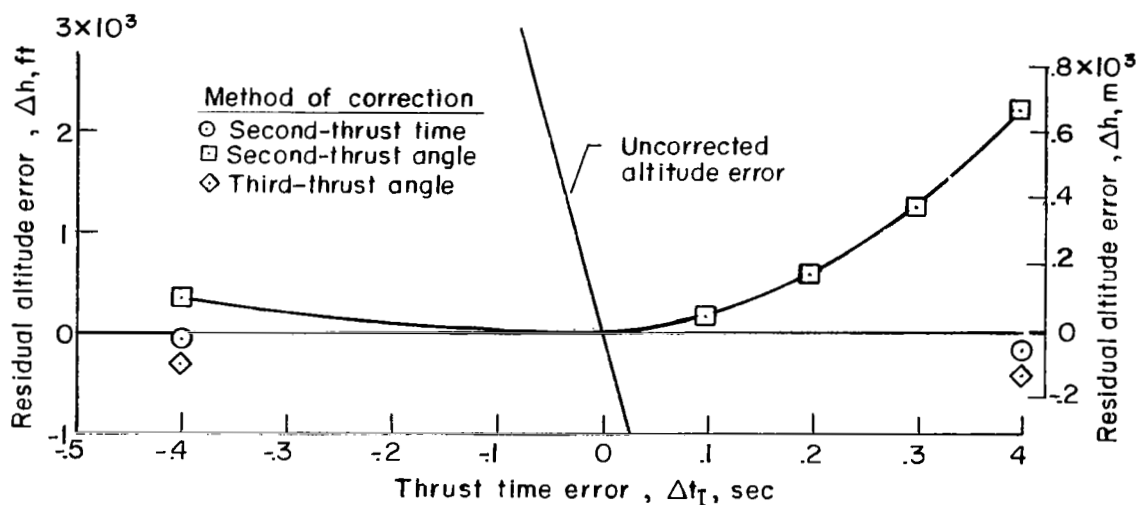


Figure 10.- Residual altitude errors after correction of first-thrust time errors by corrections during second and third thrust periods.

The results of some computations using these coefficients to correct for definite time and angle errors imposed during the first thrust period are presented in figures 10 and 11, and summarized in table II. These show the improvement that can be obtained for an individual error.

In order to evaluate the benefit to be obtained by using these corrections in trajectories where the errors are random in magnitude and can be made throughout the trajectory, these correction coefficients were inserted into the basic computation. Pilot 18 ($\sigma_a = 0.20^\circ$; $\sigma_t = 0.20$ sec) was chosen as the example, and the correction scheme used was as follows:

1. For both angle and time errors made during the first thrust, a new nominal second-thrust time was computed by adjusting the cutoff time.
2. For both angle and time errors made during the second thrust, a new nominal third-thrust angle was computed.
3. Errors incurred during the third thrust remained uncorrected since there was no subsequent thrust period in which corrections could be made.

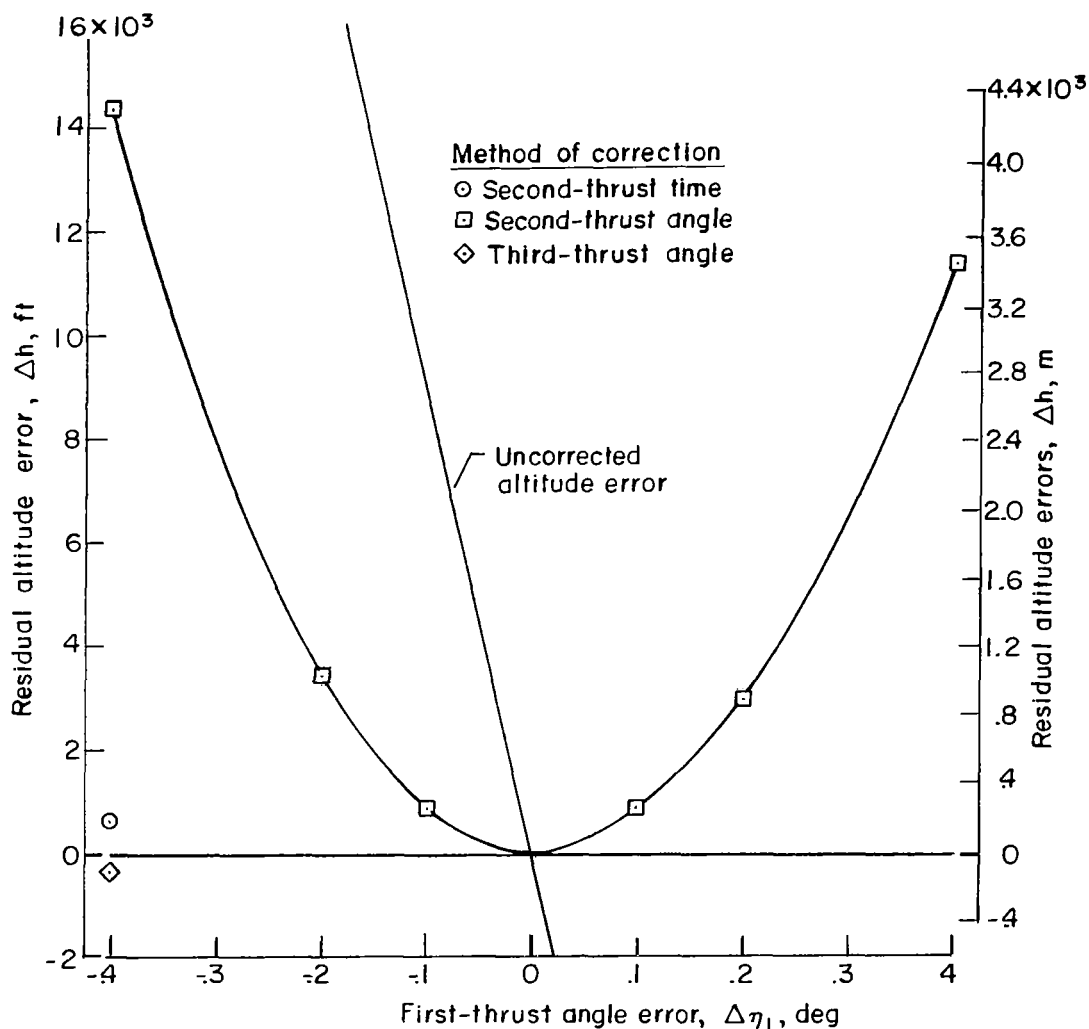


Figure 11.- Residual altitude errors after correction of first-thrust angle error by corrections during second and third thrust periods.

TABLE II.- EFFECTIVENESS OF COMPENSATING FOR TERMINAL ALTITUDE ERRORS

Procedural error		Error in h due to procedural error		Compensating adjustment			Estimate of error in corrected terminal altitude	
Δt_I , sec	$\Delta \eta_1$, deg	feet	meters	Δt_{II} , sec	$\Delta \eta_2$, deg	$\Delta \nu$, deg	feet	meters
+0.4	0	-15 240	-4 645.1	0	-5.06	0	2 200	670.6
+2	0	-7 620	-2 322.6	0	-2.53	0	550	167.6
-.2	0	7 620	2 322.6	0	+2.53	0	100	30.5
-.4	0	15 240	4 645.1	0	+5.06	0	300	91.4
+0.4	0	-15 240	-4 645.1	-0.232	0	0	-200	-61.0
-.4	0	15 240	4 645.1	+.232	0	0	-100	-30.5
+.4	0	-15 240	-4 645.1	0	0	-1.08	-400	-121.9
-.4	0	15 240	4 645.1	0	0	+1.08	-300	-91.4
0	+0.4	-37 000	-11 277.6	0	-12.28	0	11 200	3413.8
0	+2	-18 500	-5 638.8	0	-6.14	0	2 900	883.9
0	-.2	18 500	5 638.8	0	+6.14	0	3 400	1036.3
0	-.4	37 000	11 277.6	0	+12.28	0	14 300	4358.6
0	+0.4	-37 000	-11 277.6	-0.563	0	0	300	91.4
0	-.4	37 000	11 277.6	+.563	0	0	500	152.4
0	+.4	-37 000	-11 277.6	0	0	+2.61	-950	-289.6
0	-.4	37 000	11 277.6	0	0	-2.61	-400	-91.4

The results of these computations are shown in figures 4 to 8 as the solid symbols at $\sigma_a = 0.20^\circ$ and $\sigma_t = 0.20$ sec. The improvement in the final altitude is shown in figures 4 and 5; the standard error at time t_g decreased from about 25 000 ft (7620 m) to 3000 ft (914.4 m), and the number of times the vehicle hit the ground decreased from 21 to 2 in the total of 51 runs. The vertical velocity at impact also decreased significantly, from about 240 ft/sec (73.2 m/sec) to less than 160 ft/sec (48.8 m/sec). These residual errors result mainly from the control errors incurred during the third thrust period. The other end conditions – total velocity and range errors – were not significantly affected.

The results presented in figures 10 and 11 and table II show that terminal altitude errors can be substantially decreased by using the simple error-coefficient method of compensation. In addition, the results show that corrections to the second thrust time or the third thrust angle are more effective than corrections to the second thrust angle.

CONCLUDING REMARKS

An analytical study was made to assess the ability of a pilot, simulated by permissible error performance, to control the entire lunar approach and descent with relatively simple guidance schemes. The control task consisted of applying retrothrust during the hyperbolic approach to establish a lunar orbit. During this lunar coasting orbit, the lunar module was separated from the command and service module. A second deorbit thrust period was used on the lunar module to establish a coasting descent, and a final thrust period was used to put the vehicle into a reasonable landing situation. Throughout the maneuver the pilot was permitted to make reasonable errors, selected in a random manner, in the thrust time and attitude control. The control schemes consisted of maintaining a constant vehicle attitude with respect to the line of sight to the lunar horizon for the first and second thrust periods, and a constant angle with respect to the line of sight to the orbiting command and service module for the third thrust period.

The results show that a reasonably accurate pilot, one whose standard deviation in the time and angle control is within 0.1 second or degree, was required so that the final altitude and velocity errors would not become too large. Even with a pilot of these specifications, the errors were so large that the vehicle hit the ground about 20 percent of the time, with a vertical velocity as high as 260 ft/sec (79.2 m/sec), if no correction was made to the flight path.

A set of coefficients that permit correction of the final altitude error was developed. In order to use these coefficients, it is necessary to obtain a measure of the magnitude of the errors made during a thrust period so that a proper correction can be applied to the following thrust period. As an example of the corrections that could be made by means of

these coefficients, suppose that an error of 0.4° was made in the first thrust angle. This would incur a penalty of $\pm 37\ 000$ ft ($11\ 277.6$ m) in the final altitude; however, corrective measures applied during the second and third thrust periods could reduce this error to less than 1000 ft (304.8 m).

When these correction coefficients were used in the basic trajectory computation program, the final altitude errors were significantly decreased. For example, for the worst pilot (standard deviation of 0.20° and 0.20 sec) the final standard error of altitude was reduced from $25\ 000$ to 3000 ft (7620 to 914 m) and the number of surface impacts was reduced from 21 to 2 in 51 runs.

Langley Research Center,
National Aeronautics and Space Administration,
Hampton, Va., January 14, 1971.

APPENDIX A

MATHEMATICAL EQUATIONS AND METHODS USED IN THE INVESTIGATION

For this investigation all the orbits were restricted to one plane (see fig. A-1) and the vehicle was restricted to essentially three degrees of freedom, motion longitudinally and vertically and rotation for thrust alignment. This last condition was not really a degree of freedom because the thrust vector was positioned without resort to rotational dynamics.

The equations of motion used in this investigation were

$$m\ddot{x}_i = F_{X_i} - mG \cos \lambda$$

$$m\ddot{y}_i = F_{Y_i} - mG \sin \lambda$$

where F_{X_i} and F_{Y_i} are the thrust components along the X_i and Y_i axes, respectively. The direction of thrust was different for the two vehicles, being along the X_{CSM} axis for the CSM and along the $-Z_{LM}$ axis for the LM. The expressions for the thrust are then:

For the CSM,

$$F_{X_i} = F_{CSM} \sin(\xi - \lambda)$$

$$F_{Y_i} = F_{CSM} \cos(\xi - \lambda)$$

For the LM,

$$F_{X_i} = F_{LM} \cos(\xi - \lambda)$$

$$F_{Y_i} = F_{LM} \sin(\xi - \lambda)$$

The terms F_{CSM} and F_{LM} are considered to be constant.

The term G is the gravitational vector and is given by

$$G = \frac{\mu M}{R^2}$$

APPENDIX A - Continued

The instantaneous mass is given by

$$m = m_0 - \int \dot{m} dt$$

where \dot{m} is integrated during the thrust periods. The distance between the vehicles was obtained from

$$l = \sqrt{\left[(x_i)_{LM} - (x_i)_{CSM} \right]^2 + \left[(y_i)_{LM} - (y_i)_{CSM} \right]^2}$$

The radial distance from the center of the moon to either of the vehicles is

$$R = \sqrt{x_i^2 + y_i^2}$$

and the velocity of the vehicle is

$$V = \sqrt{\dot{x}_i^2 + \dot{y}_i^2}$$

Two schemes for controlling the angle ξ were used:

1. Control scheme 1 takes its cue from the lunar horizon and maintains the control angle at a constant value with respect to the trailing horizon. The angle ξ varies as the angle to the horizon varies. The angle τ between the local vertical and the horizon is shown in figure A-1(a) and was obtained from

$$\tau = \tan^{-1} \frac{R_0}{h(2R_0 + h)^{1/2}}$$

The angle from the X body axis, which is the one that the pilot uses as a reference, to the horizon is given by

$$\eta = -(90^\circ - \xi - \tau)$$

and

$$\xi = \eta + 90^\circ - \tau$$

The angle η is the angle that the pilot maintains at the specified value.

The diagram shows a curved line representing the Moon's surface. A point on the left is labeled "Center of Moon". A vertical line extends downwards from this point, labeled X_i at the bottom. A horizontal line extends to the right from the "Center of Moon", labeled Y_i at the right end. A curved line represents the "Surface". A point on the surface is labeled "Lunar module". A point further to the right on the surface is labeled "Command and service module". A line connects the "Center of Moon" to the "Lunar module". A line connects the "Lunar module" to the "Command and service module". A line connects the "Center of Moon" to the "Command and service module". A line labeled Z_{LM} is perpendicular to the surface at the "Lunar module". A line labeled X_{LM} is tangent to the surface at the "Lunar module". A line labeled Y_{LM} is perpendicular to X_{LM} . A line labeled Z_{CM} is perpendicular to the surface at the "Command and service module". A line labeled X_{CM} is tangent to the surface at the "Command and service module". A line labeled Y_{CM} is perpendicular to X_{CM} . An angle α is shown between Z_{LM} and Z_{CM} . An angle λ_{LM} is shown between the line from the "Center of Moon" to the "Lunar module" and the vertical line X_i . An angle λ_{CM} is shown between the line from the "Center of Moon" to the "Command and service module" and the vertical line X_i . An angle $\Delta\lambda$ is shown between the line from the "Center of Moon" to the "Lunar module" and the line from the "Center of Moon" to the "Command and service module". A line labeled "Local vertical" is perpendicular to the surface at the "Lunar module". A line labeled "Local horizontal" is tangent to the surface at the "Lunar module". A line labeled "Surface" is tangent to the surface at the "Lunar module". A line labeled l is the distance between the "Lunar module" and the "Command and service module".

34

APPENDIX A -- Concluded

2. Control scheme 2 takes its cue from the orbiting command module. The geometry for this control scheme is shown in figure A-1(b). The angle between the line of sight from the LM to the CSM and the local vertical is α , which is obtained from

$$\cos \alpha = \frac{R_{LM} - R_{CSM} \cos \Delta\lambda}{l}$$

The control angle ν , the angle between the X_{LM} axis of the LM and the line of sight to the CSM, is obtained from

$$\nu = \alpha - 90^\circ - \xi$$

and the thrust control angle is thus

$$\xi = \alpha - 90^\circ - \nu$$

The angle ν is the angle that the pilot maintains at the specified value.

APPENDIX B

DATA FOR THE ERROR DISTRIBUTIONS

The basic data of this study were obtained in terms of errors in the trajectory parameters at key times along the trajectory. The data presented in figures B-1 to B-5 show the distributions of the errors in altitude, velocity, and range. For pilot 18 (the worst one) the distributions are shown for several times along the trajectory (figs. B-1 and B-2). For the other pilots, however, the data are presented only for the end of the run, either the time of minimum altitude or the time that the vehicle hit the ground (figs. B-3 and B-5).

The altitude and velocity error distributions as shown in figures B-1 and B-2 for pilot 18 are at the end of the first and second thrust periods (t_2 and t_4 , respectively), at the start of the third thrust (t_5) and at the end of the run (t_6 or t_7). Near the start of the trajectory (t_2) the error distribution is reasonably close to normal, but as the trajectory proceeds the distribution becomes more nearly uniform except for the number of times the LM hits the ground. The maximum magnitude of the altitude errors increases very rapidly, progressing from about ± 4000 ft (1219.2 m) at t_2 to $\pm 18\,000$ ft (5486.5 m) at t_4 , $\pm 45\,000$ ft (13 716 m) at t_5 , and $\pm 56\,000$ ft (17 068.8 m) at t_6 . The nominal final altitude was 6465 ft (1970.5 m); therefore, any error in the negative direction larger than 6465 ft (1970.5 m) would cause the vehicle to hit the ground. This puts a lower limit on the possible altitude. The column on the left end of the scale is so high because it contains not only the errors that would normally fall in this band, but also all larger negative errors. The pattern of the velocity error distributions is similar to that of the altitude error distributions. The velocity errors are as large as 6000 ft/sec (1829 m/sec).

The distributions of the errors in altitude, velocity, and range at the end of the trajectories (times t_6 and t_7) are shown in figures B-3 to B-5 for the various pilot definitions. The data are presented to show the effect of changing σ_t for a constant magnitude of σ_a . As expected, the magnitude of the errors increases with increases in both types of permissible pilot errors. Of course, as the range of the magnitude of the errors increases and spreads out along the abscissa, the number of occurrences for each error division decreases; therefore, the error distribution gradually changes from one which is nearly normal to one that approaches a uniform distribution across the spectrum.

The error-distribution data for pilot 18 ($\sigma_a = 0.20^0$, $\sigma_t = 0.20$ sec) with the first- and second-thrust errors automatically corrected are shown in figure B-6. A comparison of this figure with figure B-1(d) shows the considerable decrease in the altitude-error range that can be achieved with such corrections.

APPENDIX B - Continued

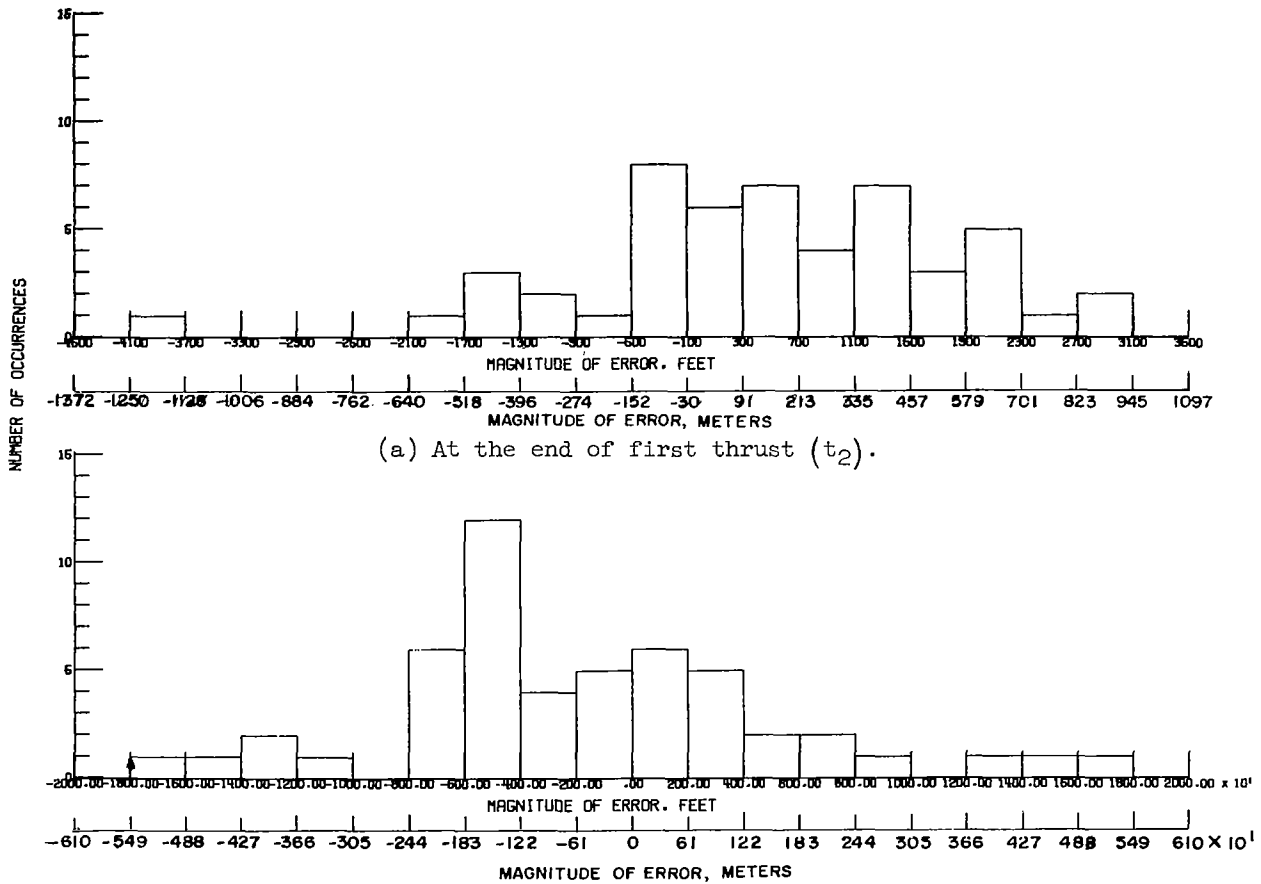
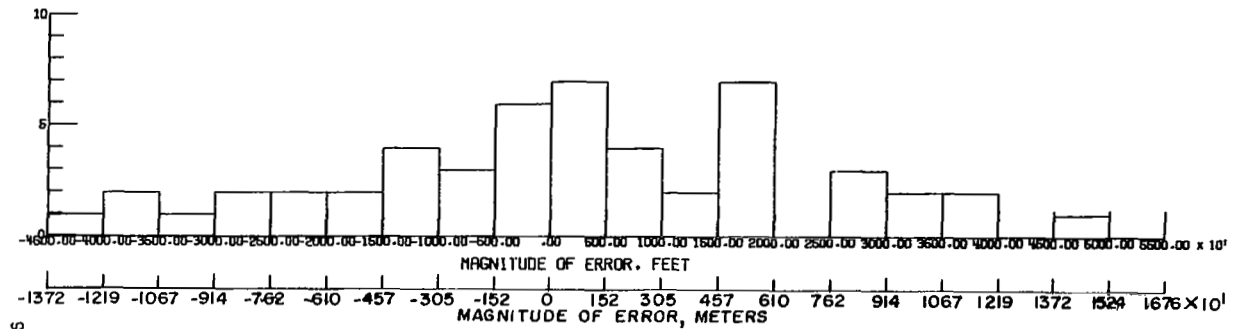
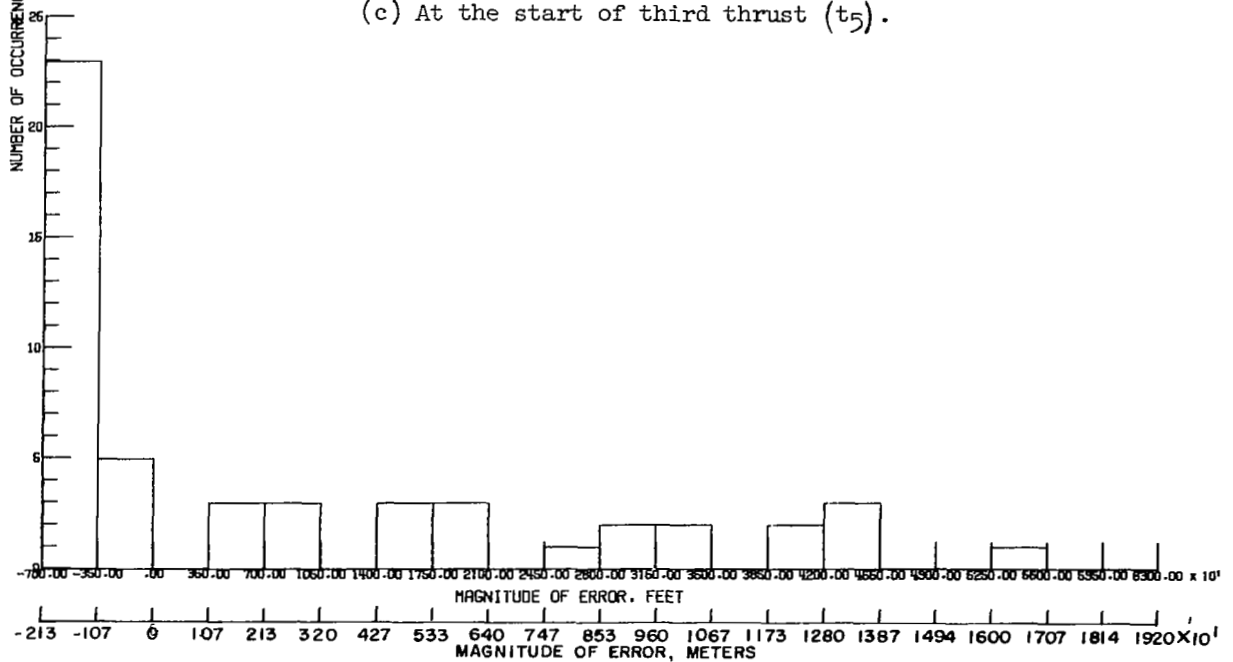


Figure B-1.- Altitude-error distributions for pilot 18 at various times along the trajectory.

APPENDIX B - Continued



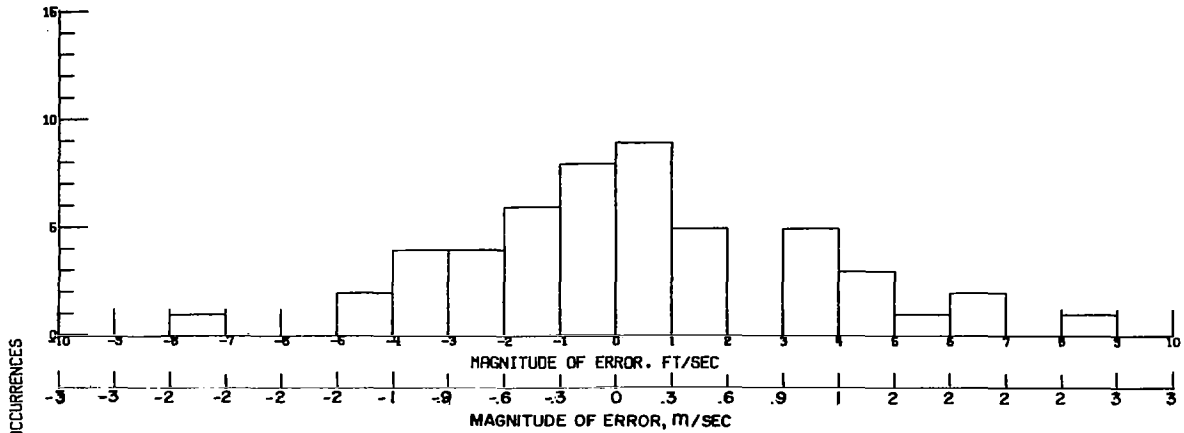
(c) At the start of third thrust (t_5).



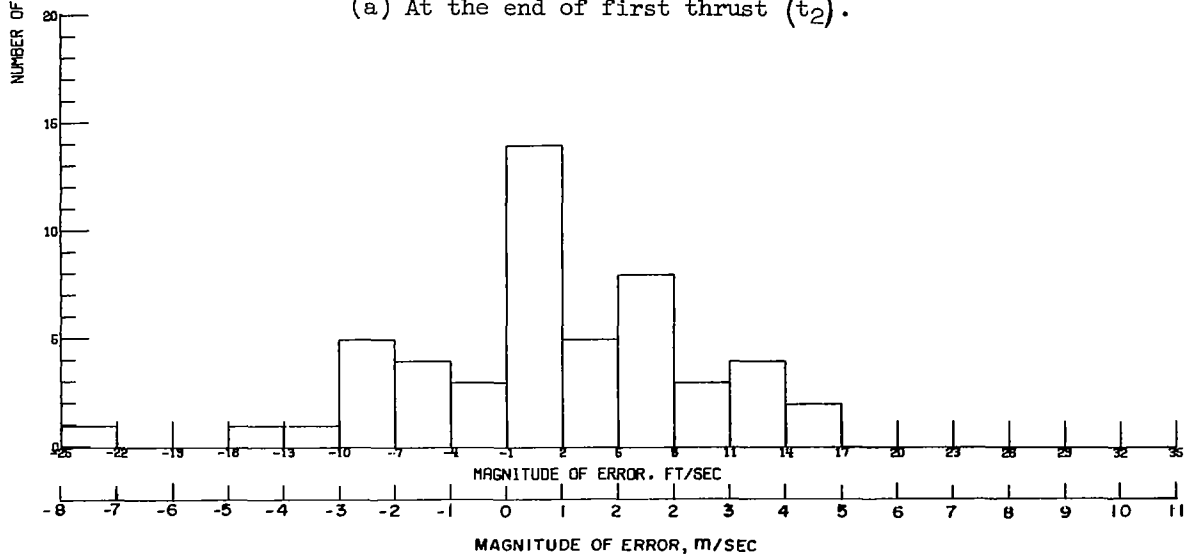
(d) At the end of the run (t_6 or t_7). The large column at the left includes the trajectories that impact the ground.

Figure B-1.- Concluded.

APPENDIX B - Continued



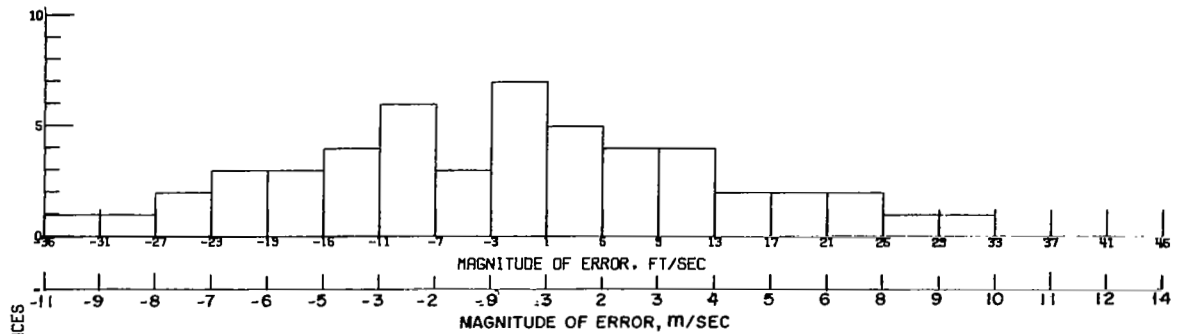
(a) At the end of first thrust (t_2).



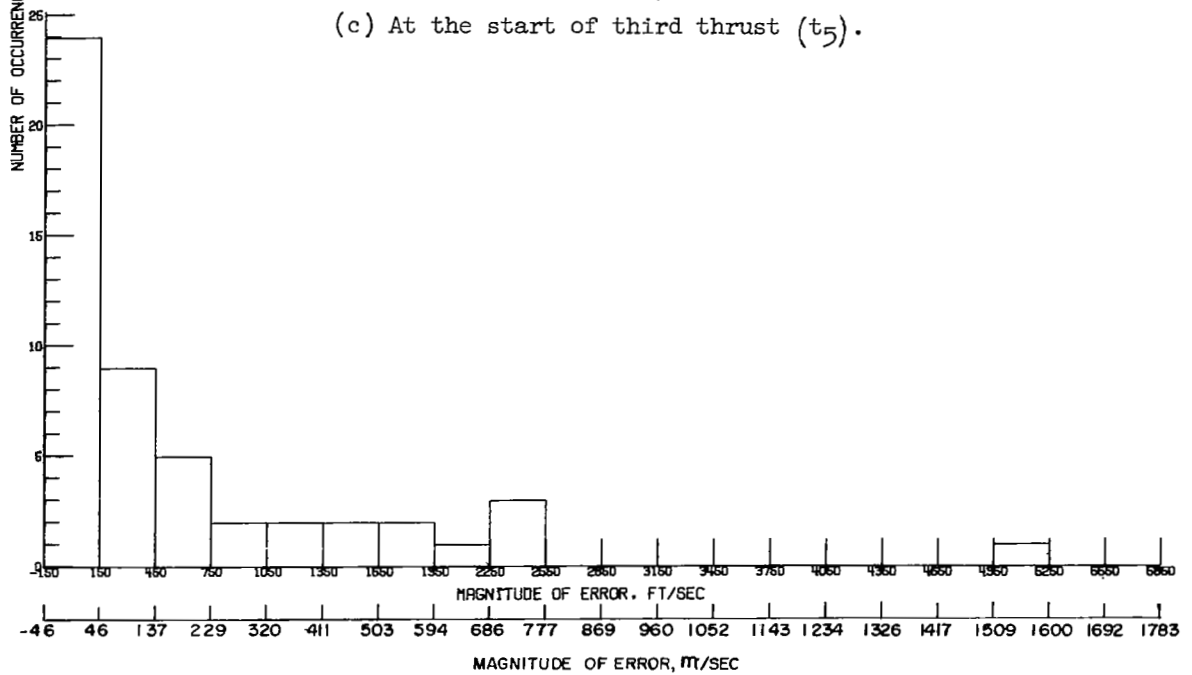
(b) At the end of second thrust (t_4).

Figure B-2.- Velocity-error distributions for pilot 18 at various times along the trajectory.

APPENDIX B -- Continued



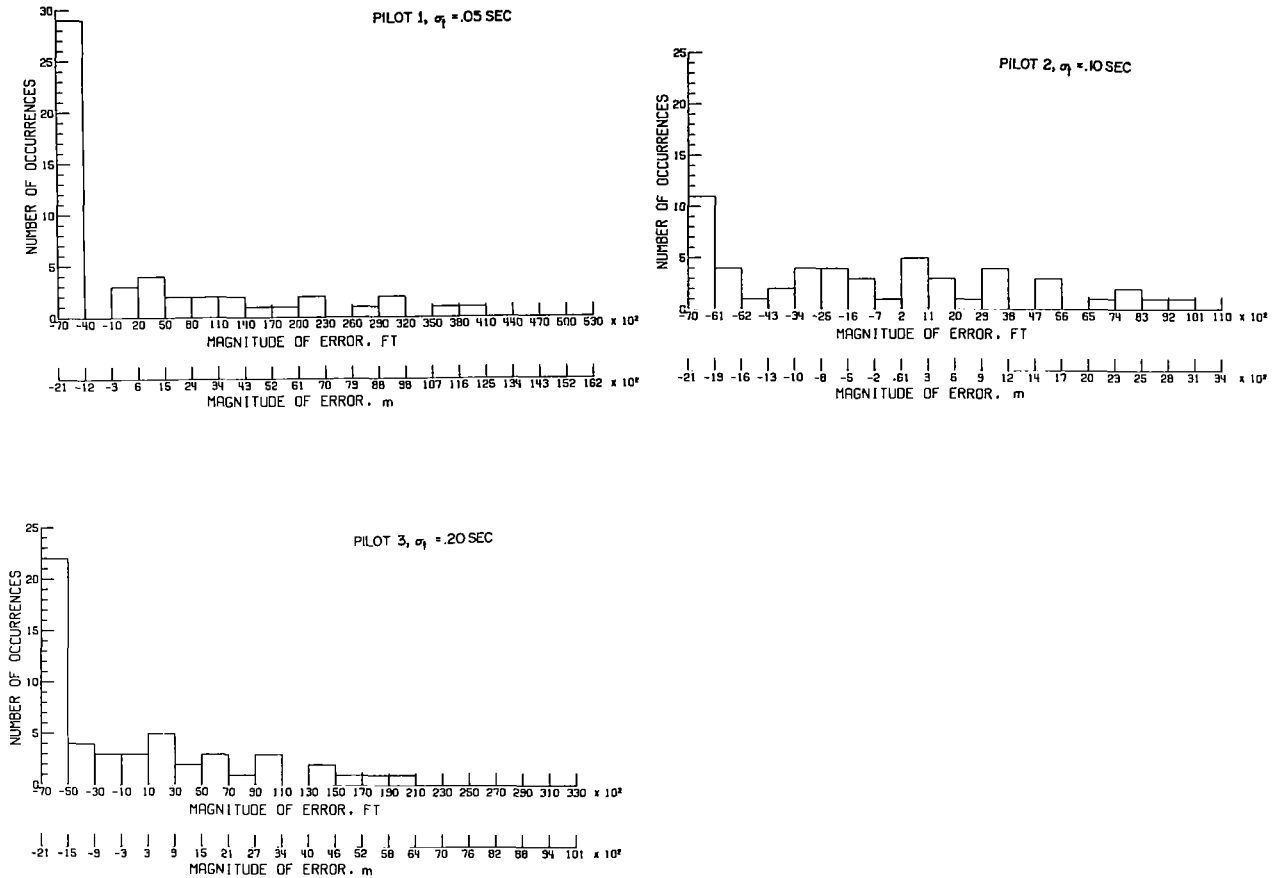
(c) At the start of third thrust (t_5).



(d) At the end of the run (t_6 or t_7).

Figure B-2.- Concluded.

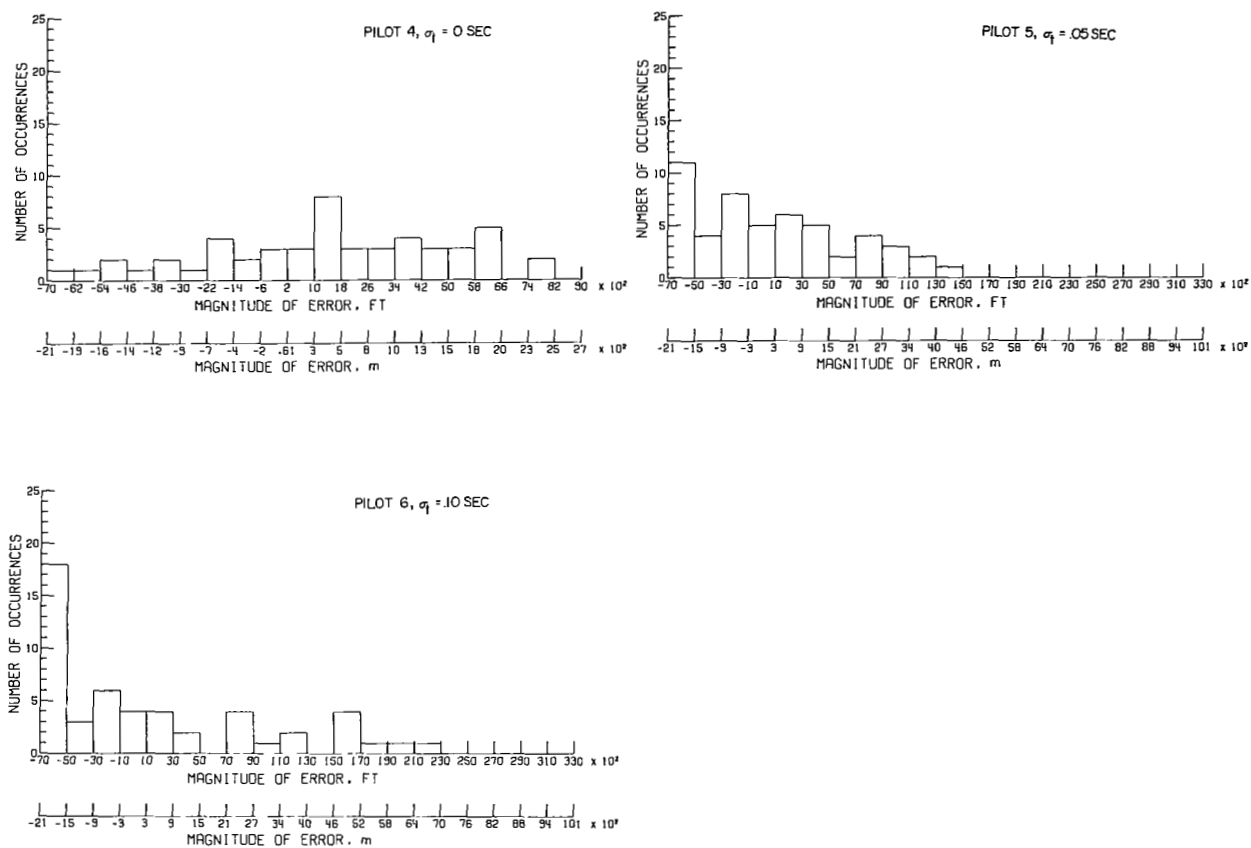
APPENDIX B – Continued



(a) Angle error definition $\sigma_a = 0^\circ$.

Figure B-3.- Altitude-error distribution at the end of the run (t_6 or t_7) for the various pilots. The large column at the left side includes the trajectories that impact the surface.

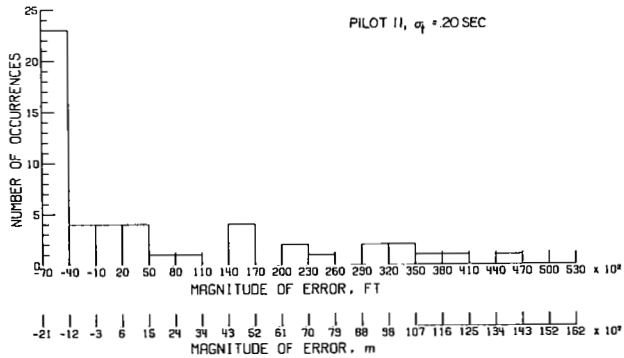
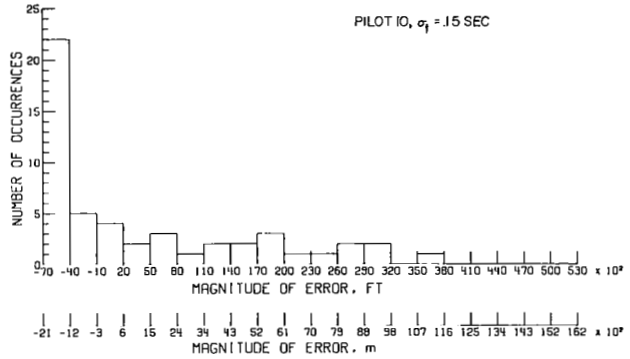
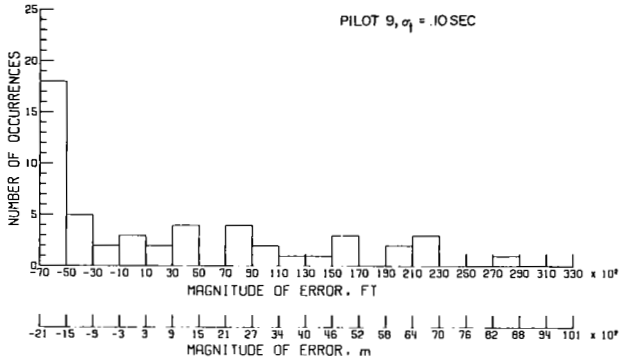
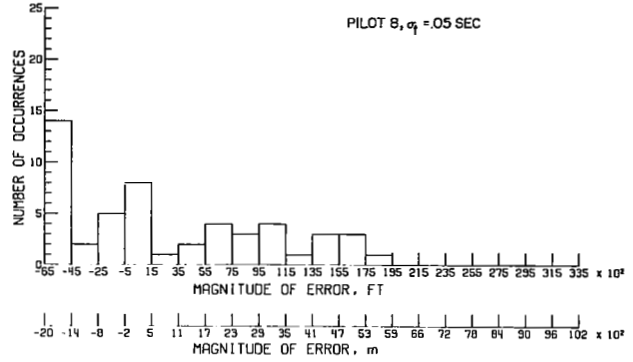
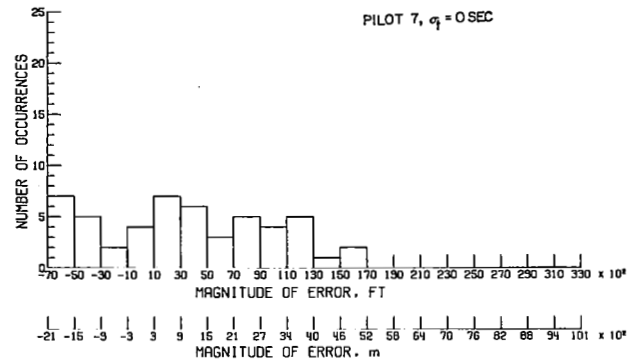
APPENDIX B -- Continued



(b) Angle error definition $\sigma_a = 0.05^\circ$.

Figure B-3.- Continued.

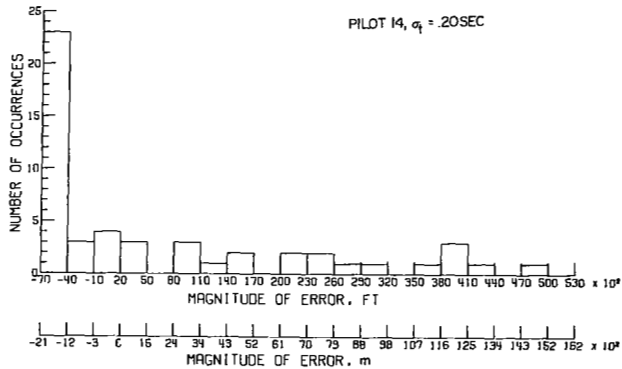
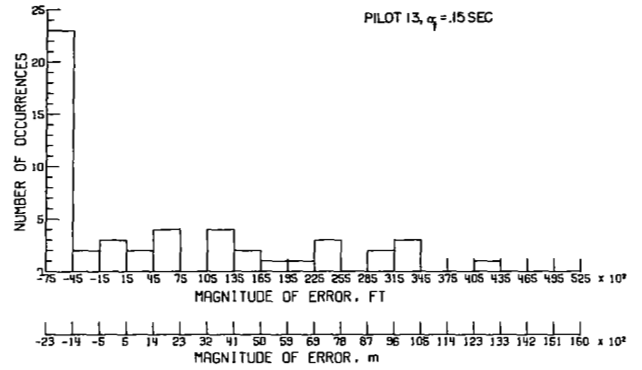
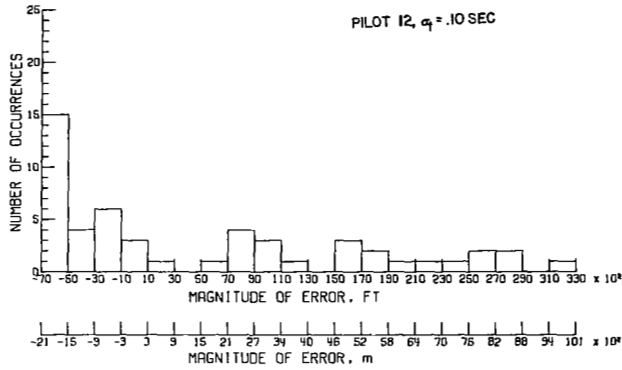
APPENDIX B – Continued



(c) Angle error definition $\sigma_a = 0.10^\circ$.

Figure B-3.- Continued.

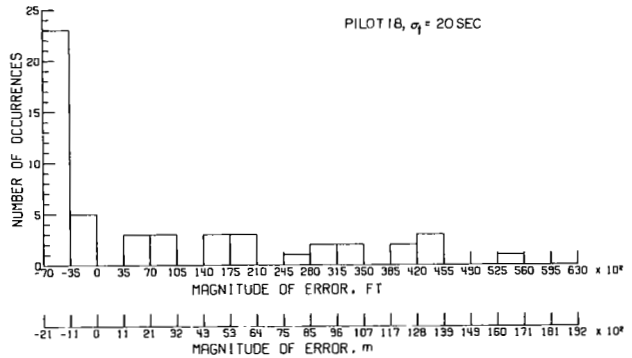
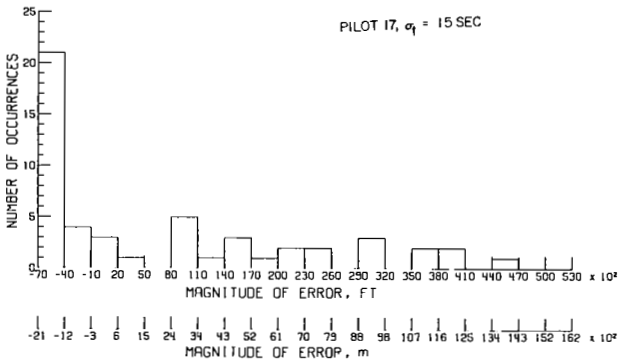
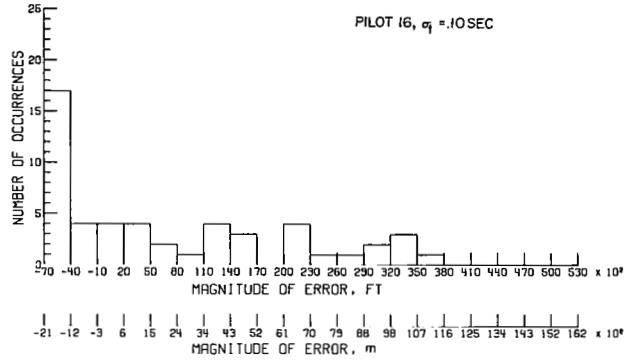
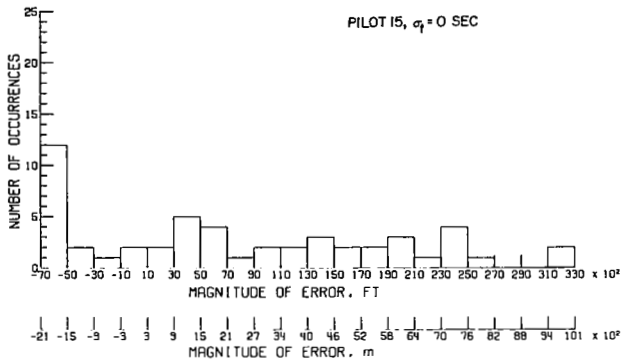
APPENDIX B – Continued



(d) Angle error definition $\sigma_a = 0.15^\circ$.

Figure B-3.- Continued.

APPENDIX B – Continued



(e) Angle error definition $\sigma_a = 0.20^\circ$.

Figure B-3.- Concluded.

APPENDIX B – Continued

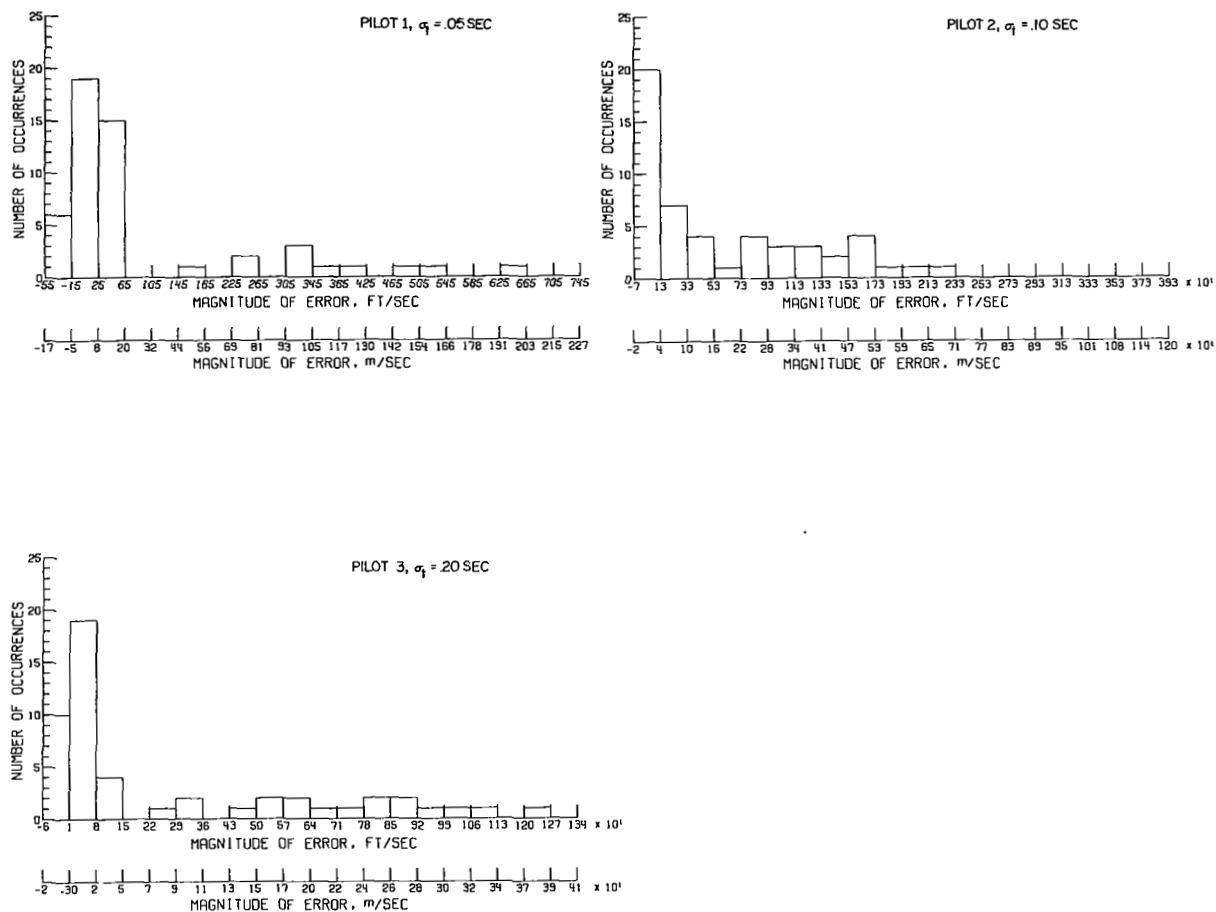
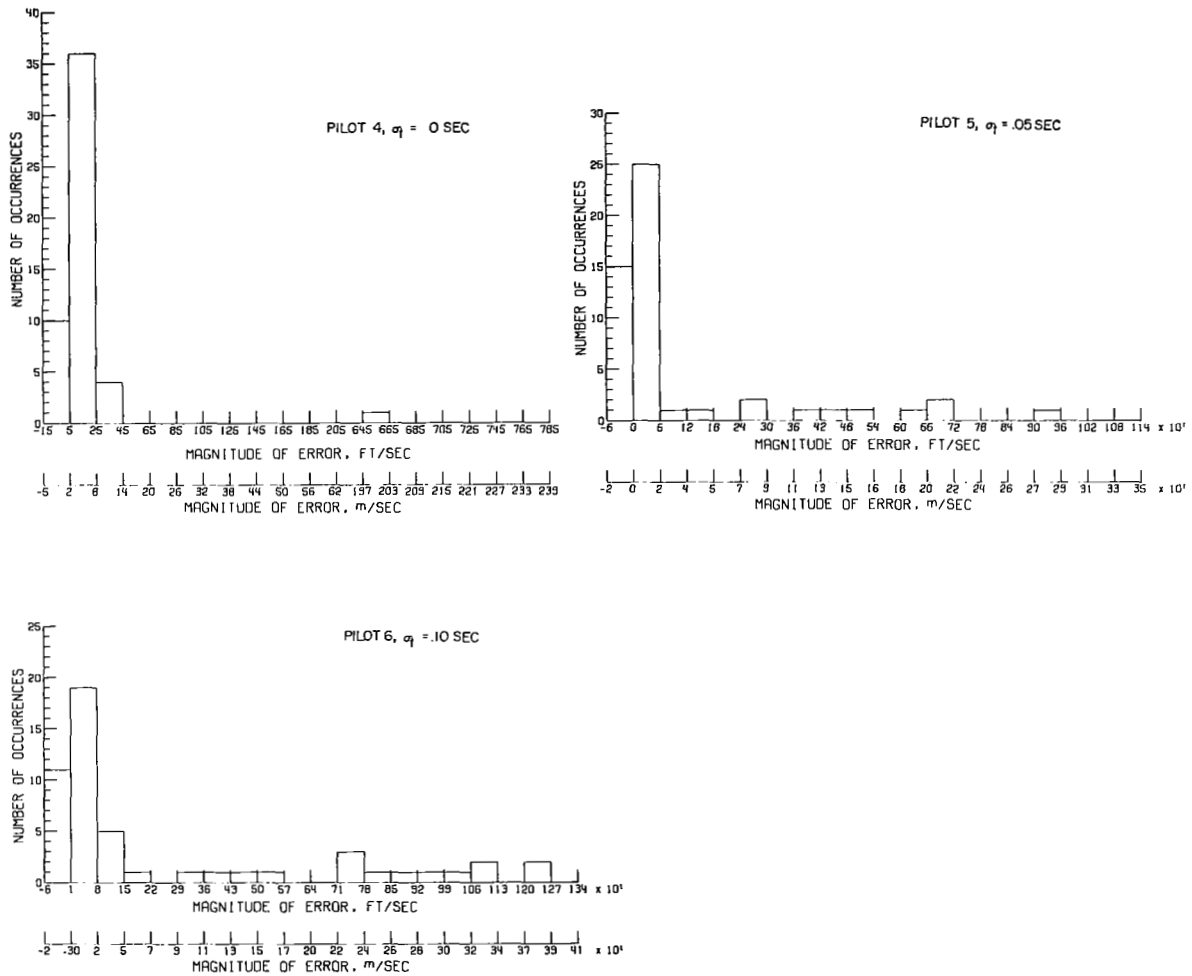


Figure B-4.- Velocity-error distributions at the end of the run (t_6 or t_7) for the various pilots.

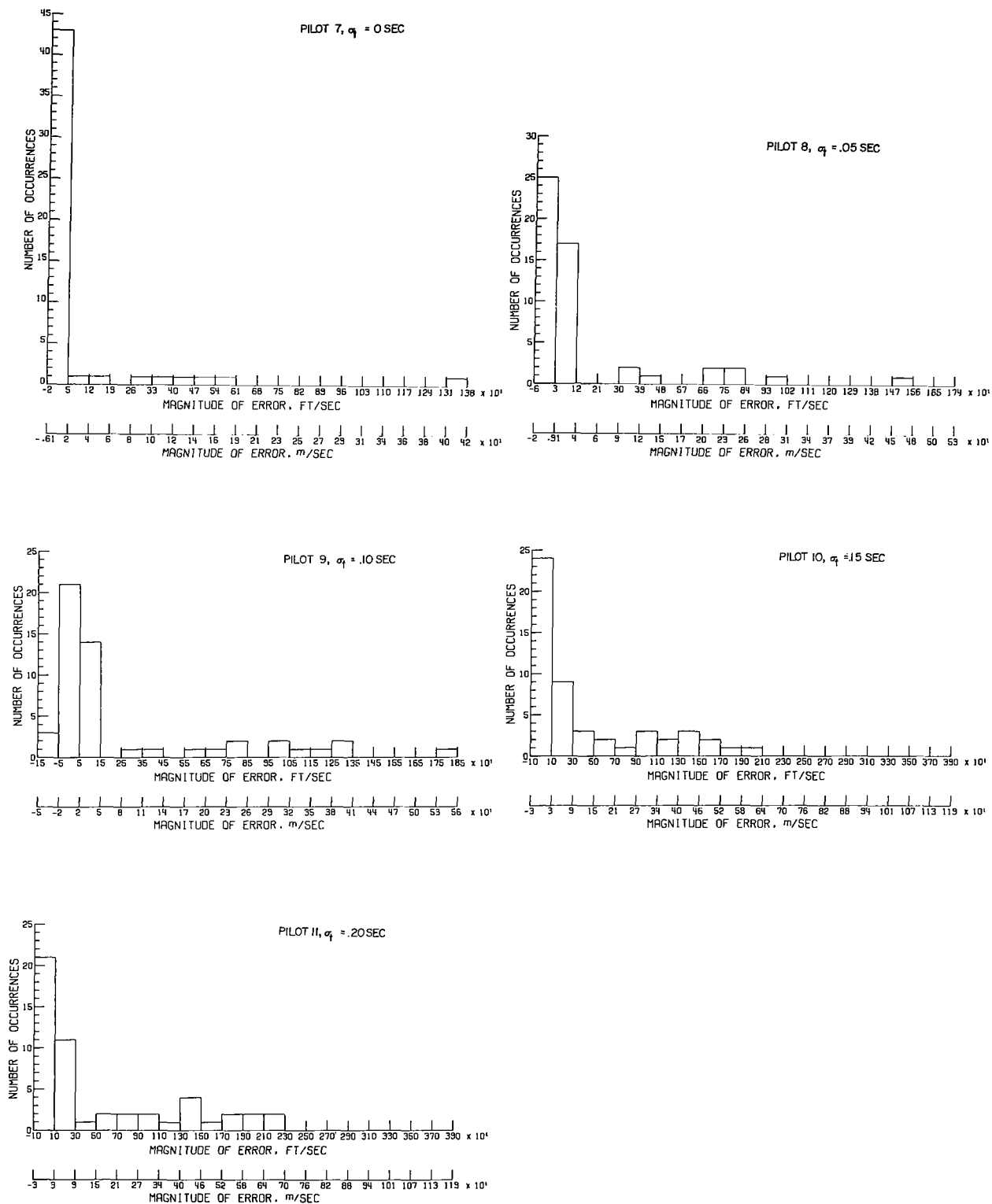
APPENDIX B – Continued



(b) Angle error definition $\sigma_a = 0.05^\circ$.

Figure B-4.- Continued.

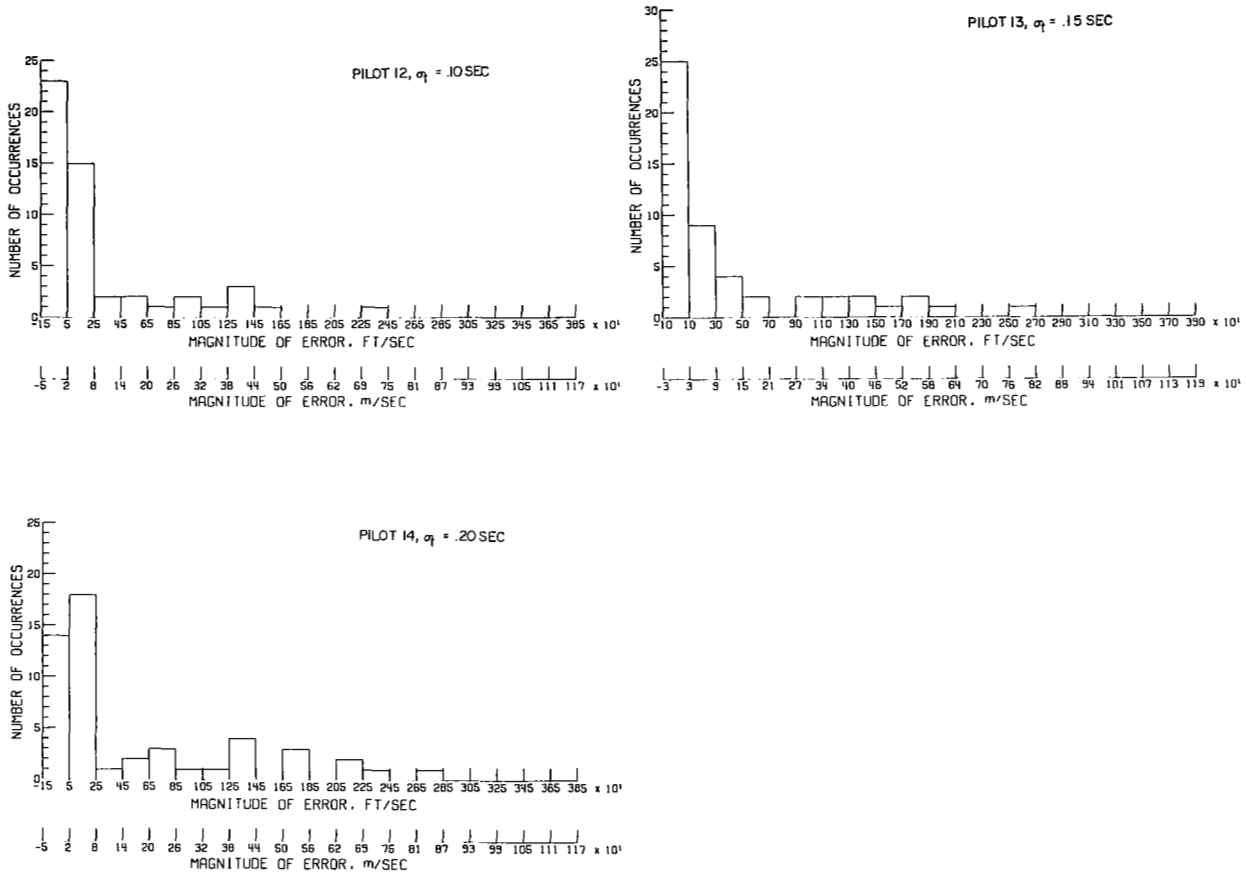
APPENDIX B – Continued



(c) Angle error definition $\sigma_a = 0.10^\circ$.

Figure B-4.- Continued.

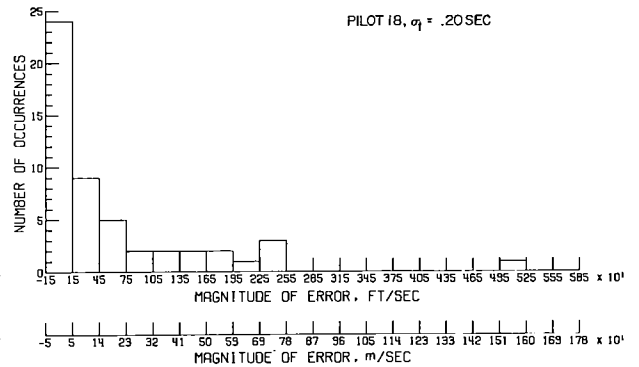
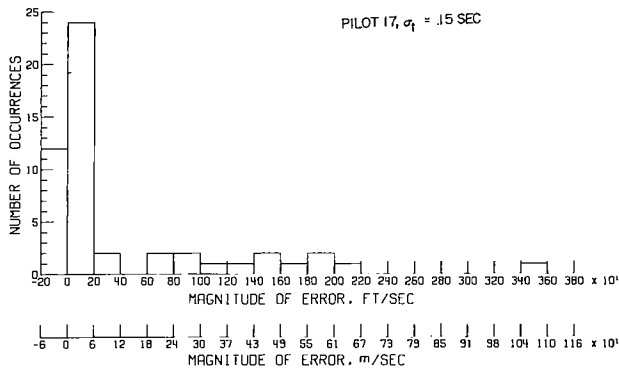
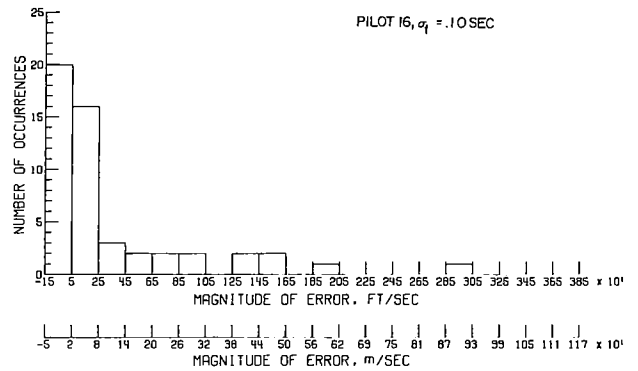
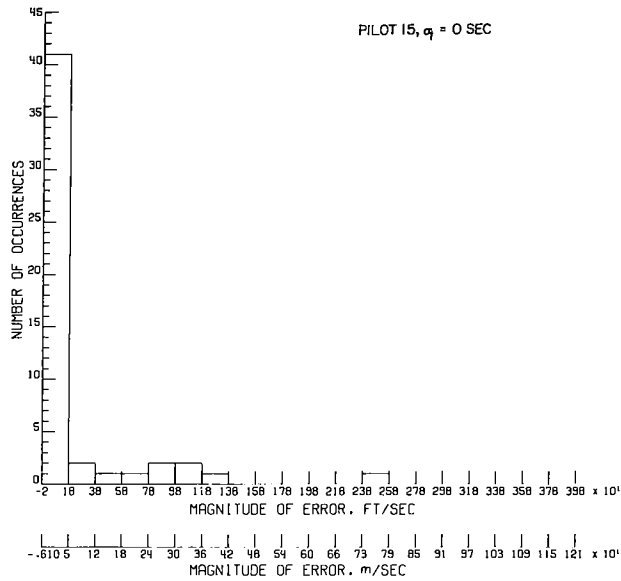
APPENDIX B – Continued



(d) Angle error definition $\sigma_a = 0.15^\circ$.

Figure B-4.- Continued.

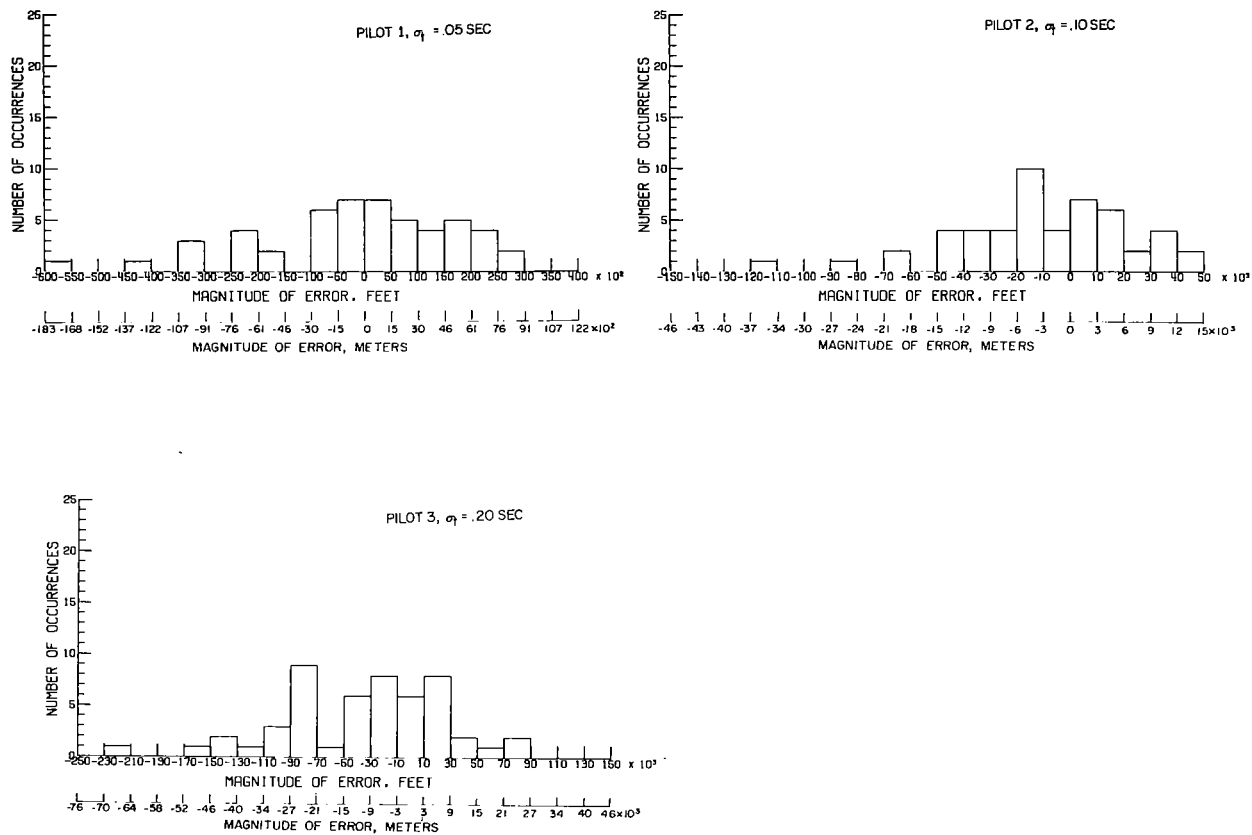
APPENDIX B – Continued



(e) Angle error definition $\sigma_a = 0.20^\circ$.

Figure B-4.- Concluded.

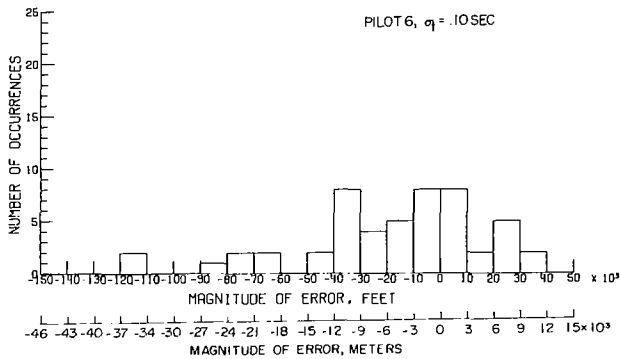
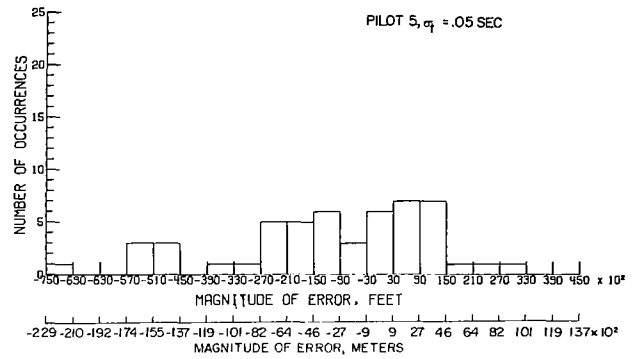
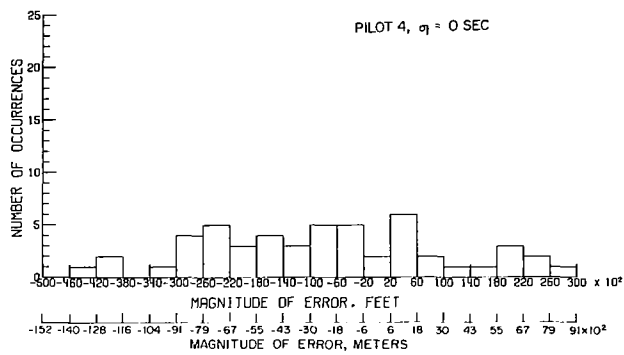
APPENDIX B – Continued



(a) Angle error definition $\sigma_a = 0^\circ$.

Figure B-5.- Range error distributions at the end of the run (t_6 or t_7) for the various pilots.

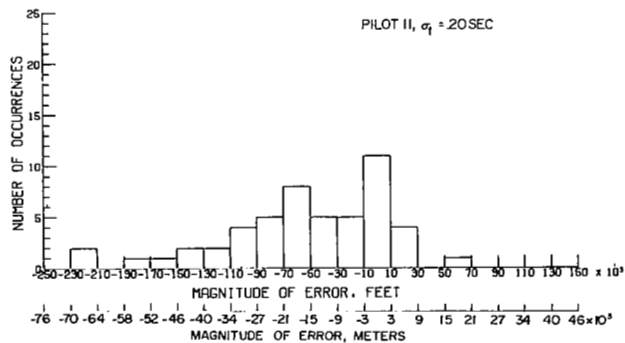
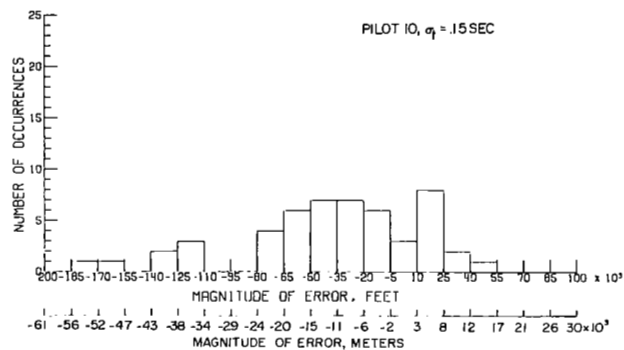
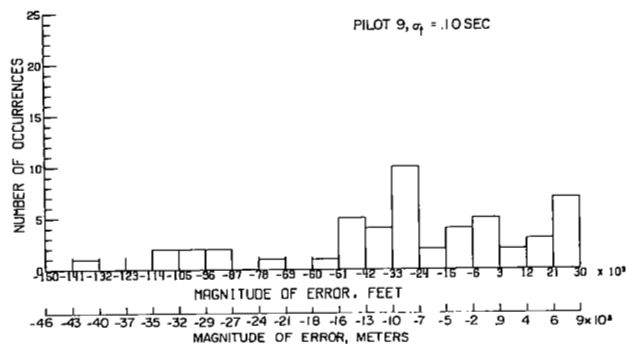
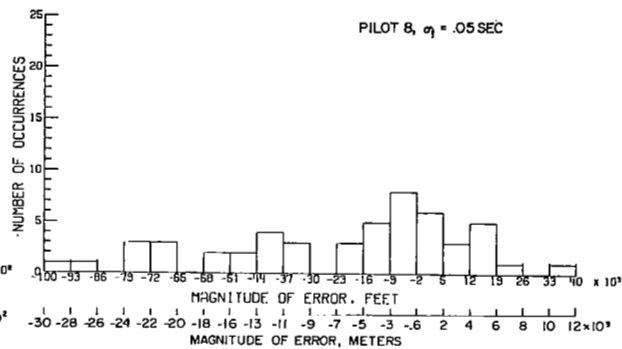
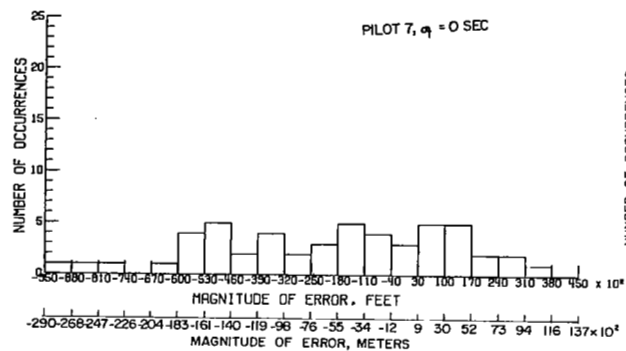
APPENDIX B - Continued



(b) Angle error definition $\sigma_a = 0.05^\circ$.

Figure B-5.- Continued.

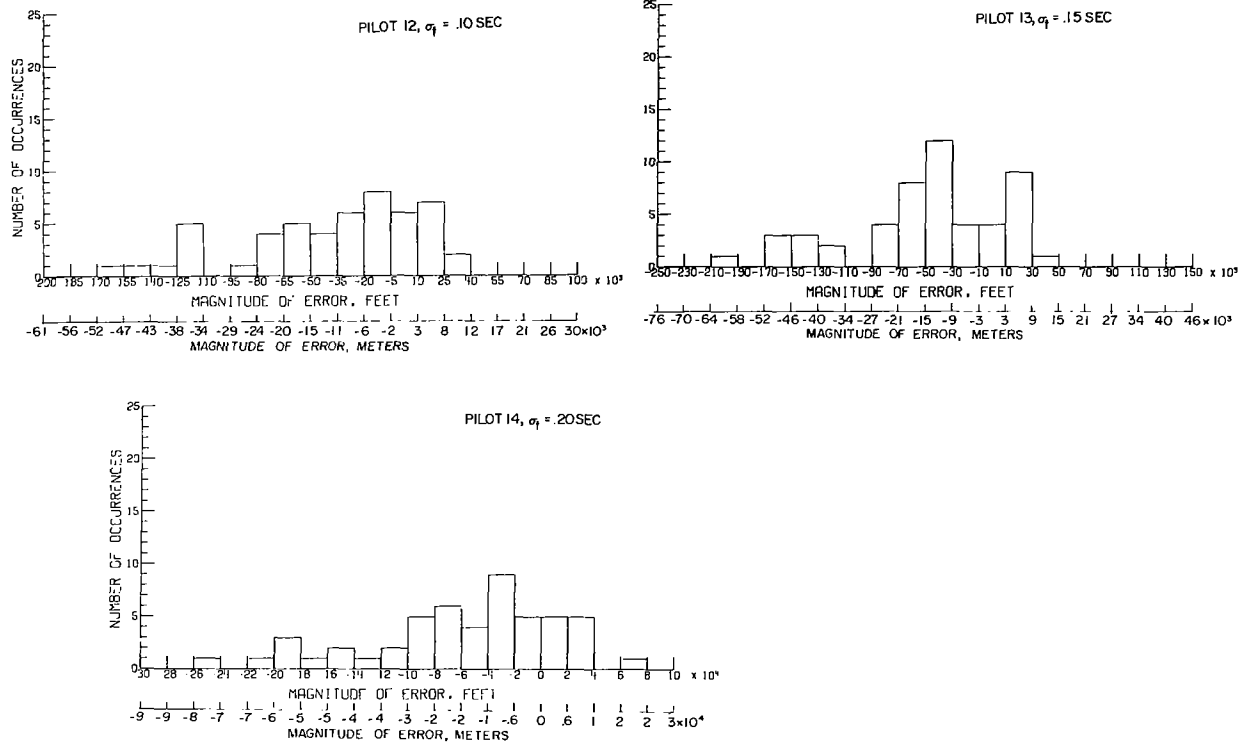
APPENDIX B - Continued



(c) Angle error definition $\sigma_a = 0.10^\circ$.

Figure B-5.- Continued.

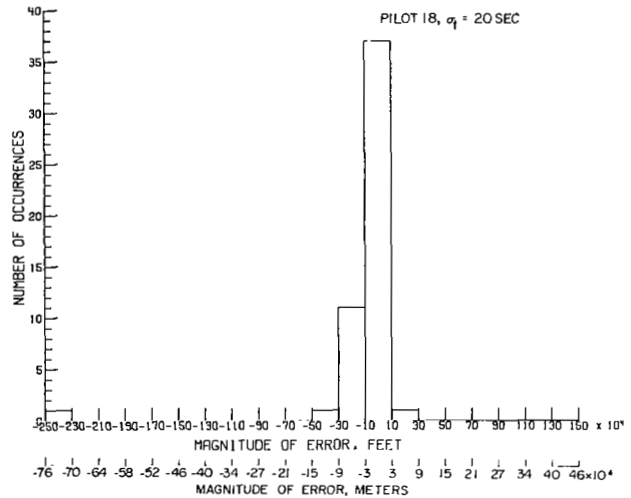
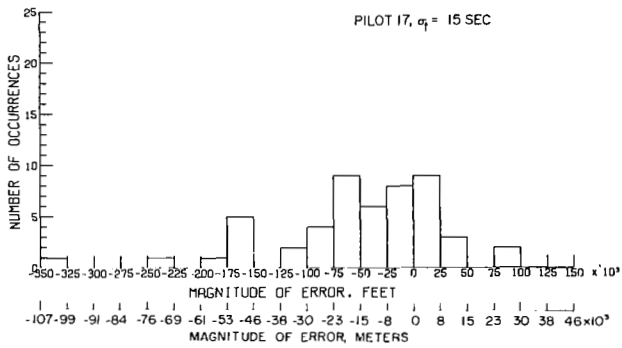
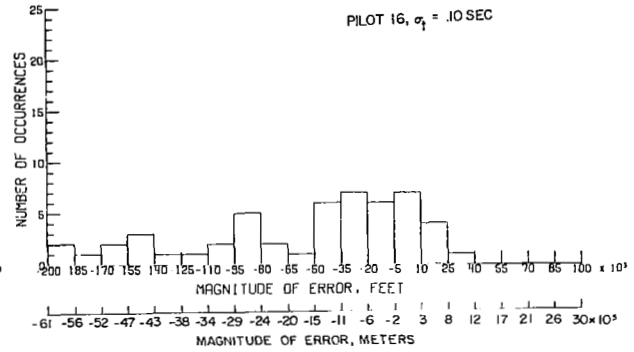
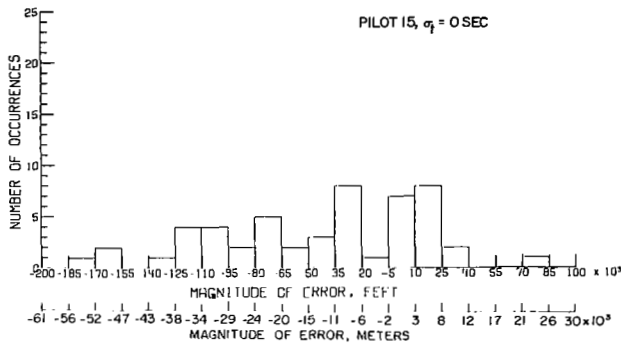
APPENDIX B – Continued



(d) Angle error definition $\sigma_a = 0.15^\circ$.

Figure B-5.- Continued.

APPENDIX B – Continued



(e) Angle error definition $\sigma_B = 0.20^\circ$.

Figure B-5.- Concluded.

APPENDIX B - Concluded

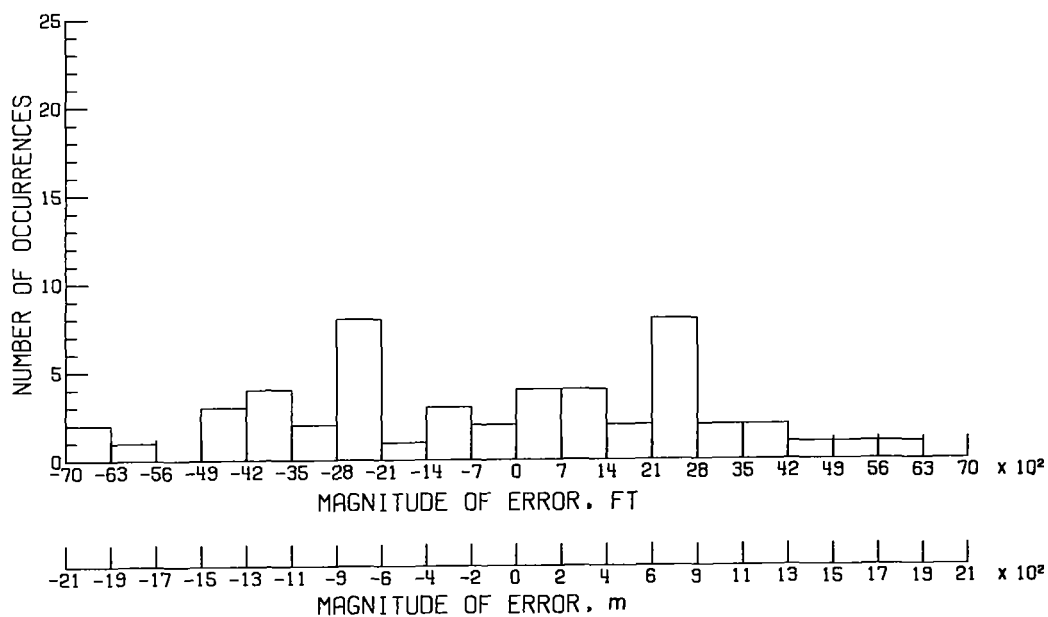


Figure B-6.- Altitude-error distributions for pilot 18 with error corrections applied for the final altitude, t_6 or t_7 .

REFERENCES

1. Miller, G. Kimball, Jr.; and Sparrow, Gene W.: Visual Simulation of Lunar Orbit Establishment Using a Simplified Guidance Technique. NASA TN D-3524, 1966.
2. Miller, G. Kimball, Jr.; and Fletcher, Herman S.: Simulator Study of Ability of Pilots to Establish Near-Circular Lunar Orbits Using Simplified Guidance Techniques. NASA TN D-2631, 1965.
3. Barker, L. Keith; and Sparrow, Gene W.: An Analytical Investigation of a Simplified Thrust-Vector Orientation Technique for Establishing Lunar Orbits. NASA TN D-3296, 1966.
4. Miller, G. Kimball, Jr.; and Fletcher, Herman S.: Fixed-Base-Simulator Study of Ability of Pilots to Perform Soft Lunar Landings by Using a Simplified Guidance Technique. NASA TN D-2993, 1965.
5. Miller, G. Kimball, Jr.: A Manual Navigation Method for Evaluating Transfer Orbits for Lunar Landings. NASA TN D-4756, 1968.
6. Silva, Robert M.; and Mills, Jon Gary: Analytic Development of Optimum Astronaut Procedures for Use of the Air Force Space Navigation System in the Manual Mode. AFAL-TR-69-14, U.S. Air Force, Sept. 1969.